VTT TIEDOTTEITA

Martin Bojinov, Timo Laitinen, Pekka Moilanen, Kari Mäkelä, Matti Mäkelä, Timo Saario & Pekka Sirkiä

Development of a controlled-distance electrochemistry arrangement to be used in power plant environments

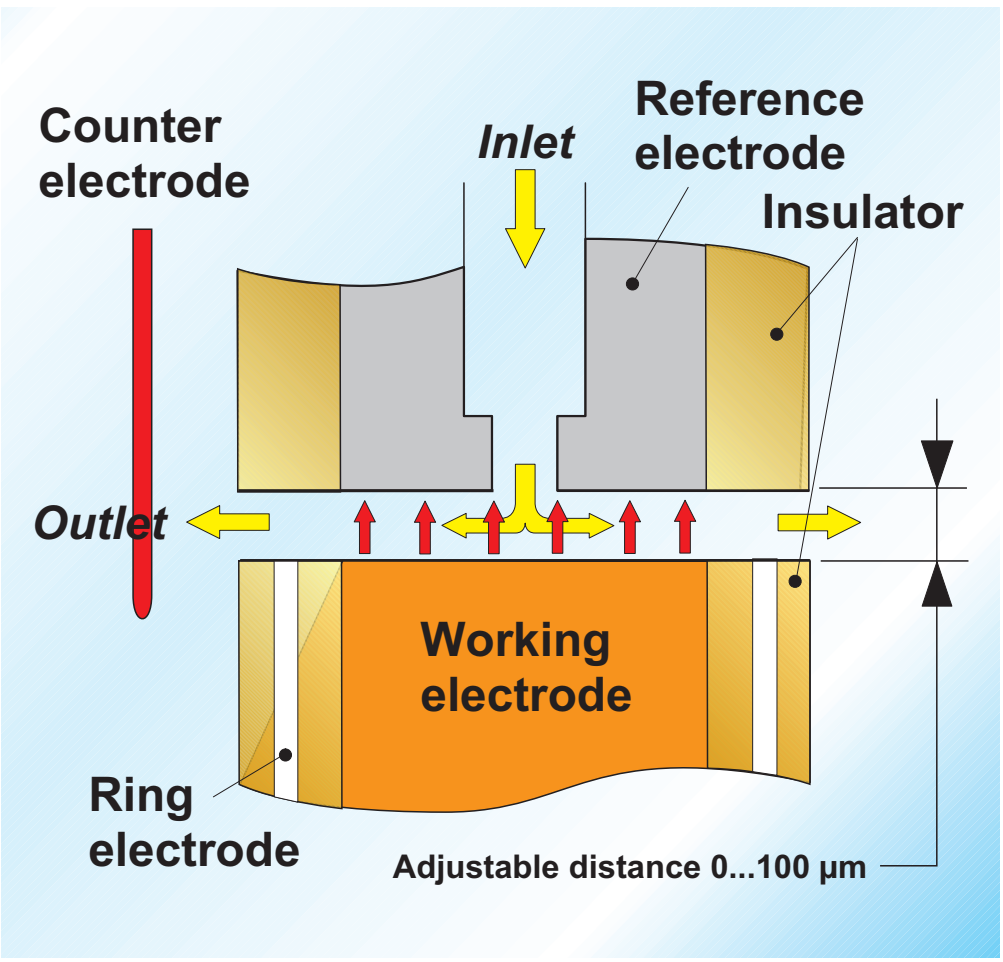

TECHNICAL RESEARCH CENTRE OF FINLAND

ESPOO 2000

VTT TIEDOTTEITA – MEDDELANDEN – RESEARCH NOTES 2039

Development of a controlled-distance electrochemistry arrangement to be used in power plant environments

Martin Bojinov, Timo Laitinen, Pekka Moilanen,
Kari Mäkelä, Matti Mäkelä, Timo Saario & Pekka Sirkiä

VTT Manufacturing Technology

TECHNICAL RESEARCH CENTRE OF FINLAND
ESPOO 2000

ISBN 951–38–5681–X (soft back ed.)
ISSN 1235–0605 (soft back ed.)

ISBN 951–38–5682–8 (URL:http://www.inf.vtt.fi/pdf)
ISSN 1455–0865 (URL:http://www.inf.vtt.fi/pdf)

JULKAISIJA – UTGIVARE – PUBLISHER

Valtion teknillinen tutkimuskeskus (VTT), Vuorimiehentie 5, PL 2000, 02044 VTT
puh. vaihde (09) 4561, faksi (09) 456 4374

Statens tekniska forskningscentral (VTT), Bergsmansvägen 5, PB 2000, 02044 VTT
tel. växel (09) 4561, fax (09) 456 4374

Technical Research Centre of Finland (VTT), Vuorimiehentie 5, P.O.Box 2000, FIN–02044 VTT, Finland
phone internat. + 358 9 4561, fax + 358 9 456 4374

VTT Valmistustekniikka, Voimalaitosten materiaalitekniikka, Kemistintie 3, PL 1704, 02044 VTT
puh. vaihde (09) 4561, faksi (09) 456 7002, (09) 456 5875

VTT Tillverkningsteknik, Material och strukturell integritet, Kemistvägen 3, PB 1704, 02044 VTT
tel. växel (09) 4561, fax (09) 456 7002, (09) 456 5875

VTT Manufacturing Technology, Materials and Structural Integrity,
Kemistintie 3, P.O.Box 1704, FIN–02044 VTT, Finland
phone internat. + 358 9 4561, fax + 358 9 456 7002, + 358 9 456 5875

Otamedia Oy, Espoo 2000

Bojinov, Martin, Laitinen, Timo, Moilanen, Pekka, Mäkelä, Kari, Mäkelä, Matti, Saario, Timo & Sirkiä, Pekka. Development of a controlled-distance electrochemistry arrangement to be used in power plant environments. Espoo 2000, Technical Research Centre of Finland, VTT Tiedotteita – Meddelanden – Research Notes 2039. 47 p.

Keywords controlled-distance electrochemistry, CDE, nuclear power plants, high temperatures, corrosion, measurement, fuel cladding, oxide films, water, experimentation, TLEC

Abstract

This publication presents the state-of-the-art of the controlled-distance electrochemistry (CDE) arrangement developed at VTT. Due to the possibility to control accurately the distance between two electrodes, the CDE arrangement makes possible electrochemical measurements in poorly-conductive media such as simulated coolants of light water reactor systems. This experimental arrangement has now been developed into a versatile electrochemical tool, which can be used for thin-layer electrochemistry (TLEC), wall-jet ring-disc and contact electric impedance (CEI) as well as contact electric resistance (CER) measurements. This report comprises results from the years 1997–1999 and summarises the different possible TLEC configurations and electrode locations as well as the development of a bellows-driven CDE arrangement.

Preface

The work reported in this publication has been carried out as a part of the Research Programme on Operational Safety and Structural Integrity 1999–2002, FINNUS. The development of electrochemical techniques for high-temperature aqueous environments corresponding to coolant conditions in nuclear power plants is one of the subtasks of the Ageing phenomena (AGE) project in FINNUS. The financial support from the Finnish Ministry of Trade and Industry, the Radiation and Nuclear Safety Authority, Finland and OECD Halden Reactor Project, Norway, is gratefully acknowledged.

Contents

1. Introduction

The susceptibility of construction materials to general and localised corrosion in high-temperature aqueous environments and the corrosion of fuel cladding in nuclear power plants is greatly influenced by the electric and electrochemical properties of the oxide films forming on material surfaces. In addition, activity build-up on primary circuit surfaces is closely related to the properties of the grown-on and deposited oxide films. To minimise the risks of corrosion and activity build-up, the mechanisms of phenomena taking place on oxide surfaces and within oxide films need to be modelled and understood. This in turn calls for more experimental information and thus necessitates the development of new experimental techniques and procedures capable of operating *in situ* in high temperature aqueous environments.

The contact electric resistance (CER) technique has been developed at VTT during the 1990's as the first step to characterise the electric properties of oxide films in high-temperature high-pressure environments [1]. Due to the possibility to control accurately the distance between two electrodes, the CER system has been found to offer versatile possibilities for other types of electrochemical measurements as well. It for instance makes possible electrochemical measurements in poorly-conductive media such as simulated LWR coolants. The low conductivity of the aqueous coolant complicates conventional electrochemical studies on construction and fuel cladding materials. This can be overcome by means of a thin-layer electrochemistry (TLEC) arrangement based on the CER system. This TLEC arrangement has been introduced by VTT in 1998, and its applications to various electrochemical measurements have already been described in several communications [2–8].

This experimental arrangement has now been developed into a versatile tool, which we call a controlled-distance electrochemistry (CDE) arrangement. It can be used for TLEC measurements, wall-jet ring-disc measurements and for contact electric impedance (CEI) and contact electric resistance measurements. This report comprises results from the years 1997–1999 and thus summarises the state-of-art of the CDE arrangement, including the wall-jet ring-disc technique, the different possible TLEC configurations and electrode locations as well as the development of a bellows-driven CDE system. The contact electric impedance, which is also based on the CDE arrangement, has been described in another report [9].

2. Description of the controlled-distance electrochemistry (CDE) arrangement

The CDE arrangement shown schematically in Fig. 1 can be employed for the following purposes, in addition to conventional electrochemical measurements, in which the gap between the working and reference electrodes is large:

Thin-layer electrochemistry (TLEC) measurements

- Thin-layer electrochemical impedance measurements to characterise the oxidation and reduction kinetics and mechanisms of metals as well as the properties of metal oxide films even in low-conductivity aqueous environments.

- Other controlled potential and controlled current measurements in low-conductivity aqueous environments

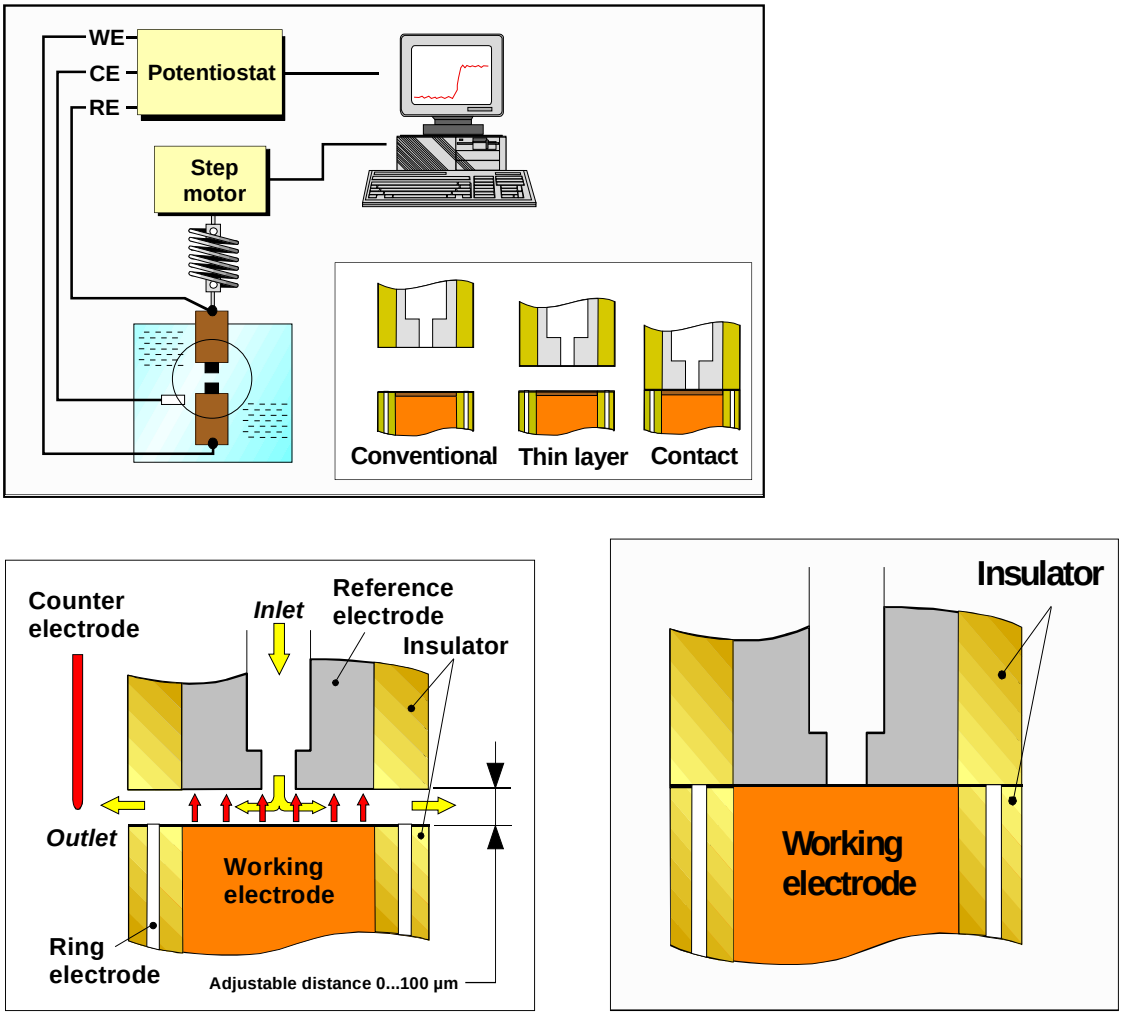

Figure 1. A scheme of the controlled-distance electrochemistry (CDE) arrangement and its different applications.

Wall-jet ring-disc measurements

- Detection of soluble species released from the studied material. In this case the concept of a working electrode is used for the combination of a disc electrode made of the studied material and a Pt ring electrode insulated electrically from the disc.
- Influence of flow rate on electrode reactions.

Solid contact measurements

- Contact electric resistance (CER) technique [1] to investigate and/or to monitor the electronic properties of surface films.
- Contact electric impedance (CEI) measurements [9] to measure the solid contact impedance spectra of oxide films.

3. Optimisation of the electrode configuration in TLEC measurements

3.1 Objective

The aim of the work described in this chapter has been to optimise the geometry of the TLEC arrangement and to propose recommendations for the use of this arrangement in different low-conductivity environments. The optimisation was based on electrochemical impedance spectroscopic (EIS) measurements with the TLEC arrangement, because EIS will probably be the most widely used application area of the TLEC.

3.2 Experimental

In the standard version of the CDE arrangement for TLEC measurements, a working electrode and a reference electrode (usually made of Ir-metal) are constructed as two parallel surfaces (tips of small diameter rods). The distance between the electrodes is adjusted with an accuracy of 10^{-9} m up to about 100 μm using a step motor. A counter electrode is situated at the side of the working electrode. The small distance between the working and reference electrode makes an accurate control of the potential possible, because it suppresses the effect of the ohmic drop in the electrolyte. In an alternative modification of the TLEC arrangement the Ir tip has also been used as a counter electrode, while the reference electrode has been located outside the small gap. This configuration is suitable to certain applications, as is shown below.

The working electrodes used in the optimisation of the system configuration were made of SS AISI 316 L(NG). Pure Cu was also used in some experiments.

Part of the experiments were performed in pure water at 273 °C in a re-circulation loop and at 200 °C in a static autoclave. The rest of the experiments were conducted in 0.01 M $Na_2B_4O_7$ at 200 °C and in water containing 10000 ppb SO_4^{2-} ions (added as H_2SO_4) at 273 °C in a static autoclave.

Impedance measurements were carried out with a Solartron 1287 ECI / 1260 FRA system controlled by CorrWare / ZPlot software (Scribner Associates).

3.3 Results and discussion

3.3.1 Standard TLEC configuration: Ir as a reference electrode

Using the Ir tip as a reference electrode makes it possible to reduce the distance of the reference electrode from the working electrode to very low values. In such cases when the current passing through the working electrode is not too high, for instance in EIS measurements with a small AC amplitude at open circuit, a potentiostat will be able to cope with the high resistance between the working and counter electrodes.

The spectra measured for SS AISI 316 L(NG) (shown in Fig. 2) demonstrate that the impedance response is not sensitive to the gap between the working electrode and the Ir tip used as the reference electrode in the range 5–21 μm in pure water.

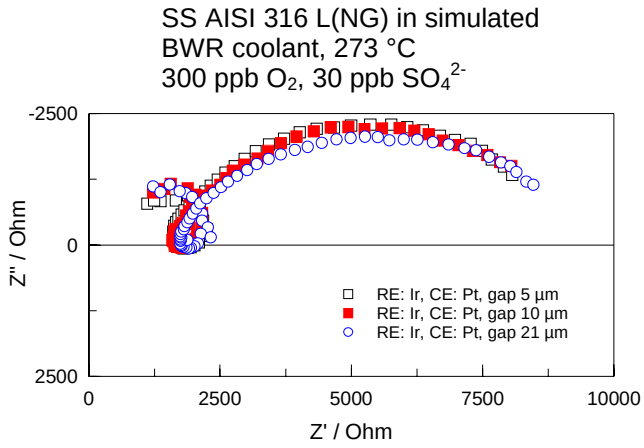

Figure 2. The influence of the distance between the working electrode and the Ir tip used as a reference electrode on the impedance spectrum of SS AISI 316 L(NG) at open circuit in simulated BWR coolant at 273 °C. Oxygen content 300 ppb. E_{corr} = 0.05 V_{SHE}.

Certain anions such as sulphates could be expected to be adsorbed on electrode surfaces or to be enriched in the thin-layer gap. Fig. 3 shows impedance spectra measured with the standard TLEC configuration in a solution containing 10000 ppb SO_4^{2-} ions ($\kappa \cong 0.1$ $mScm^{-1}$). The results obtained for SS AISI 316 L(NG) using the Ir as a reference electrode show that the distance of the Ir reference electrode from the working electrode does not influence the impedance response in the range 5–21 μm.

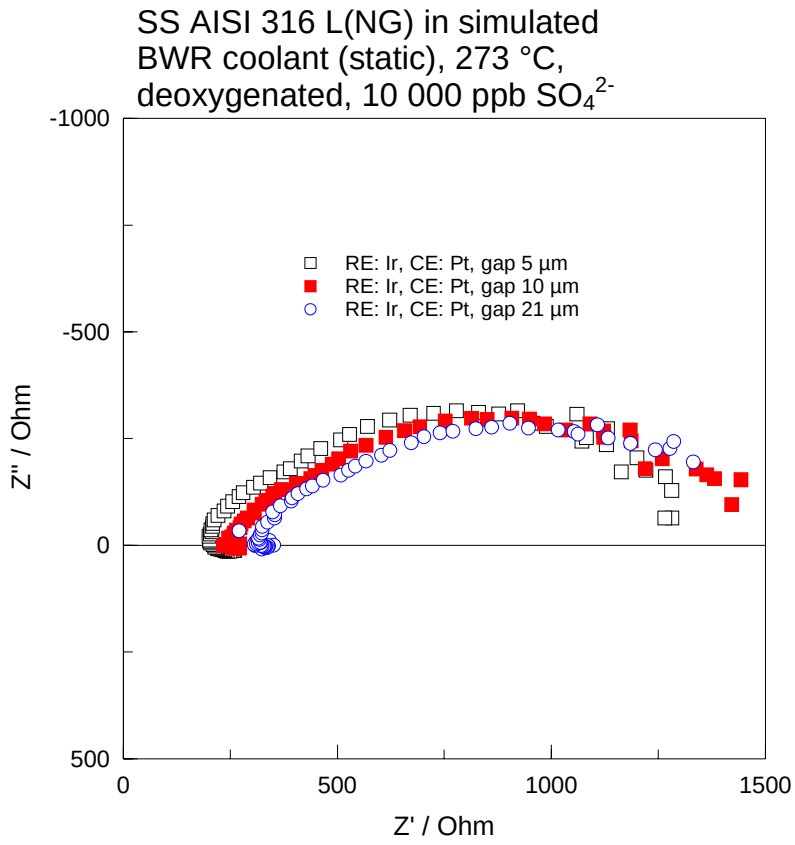

Figure 3. The influence of the distance between the working electrode and the Ir tip used as a reference electrode on the impedance spectrum of SS AISI 316 L(NG) in a deoxygenated solution containing 10000 ppb SO_4^{2-} *ions* ($\kappa \cong 0.1$ *mScm*$^{-1}$) *at 273 °C.* $E_{corr} = -0.39\ V_{SHE}$.

The impedance spectra measured for SS AISI 316 L(NG) using the thin-layer arrangement with the counter electrode at different locations (see Fig. 4) in pure water and in 0.01 M $Na_2B_4O_7$ at 200 °C are shown in Figs 5–8. The results show that neither the spectra in pure water nor in 0.01 M $Na_2B_4O_7$ are influenced by the location of the counter electrode at open circuit or under polarisation. However, during the measurements in pure water under polarisation, the potentials of the working and reference electrode were found to oscillate several hundreds of mV when measured against the frame of the autoclave. Although this seemed to have no influence on the impedance spectra, it may limit the applicability of the TLEC system in experiments under polarisation. This phenomenon may be connected with the resistive-capacitive coupling between the working, reference and counter electrodes in poorly conductive electrolytes, which has been discussed by Chechirlian et al. [10]. Further work is needed to clarify this point.

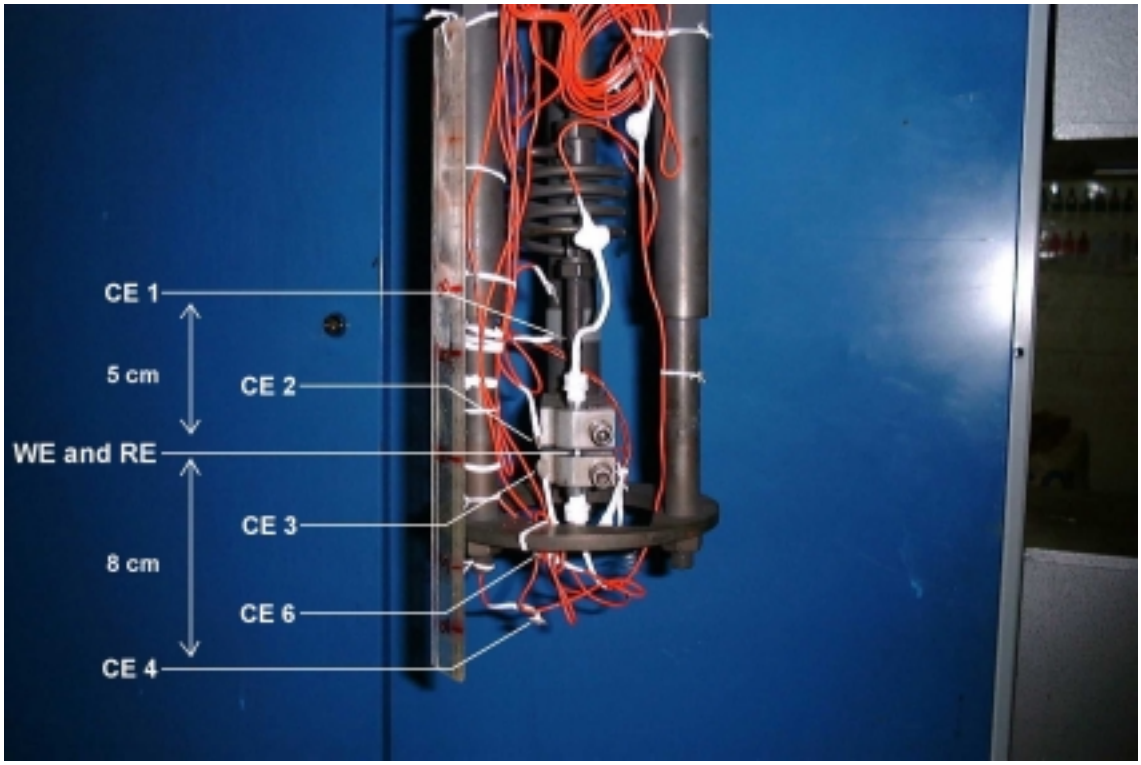

Figure 4. Different locations of the counter electrodes used in the optimisation of the electrode configuration of the thin-layer electrochemistry (TLEC) arrangement. WE = working electrode, RE = reference electrode, CE 1...CE 4 and CE 6 = counter electrodes at different locations.

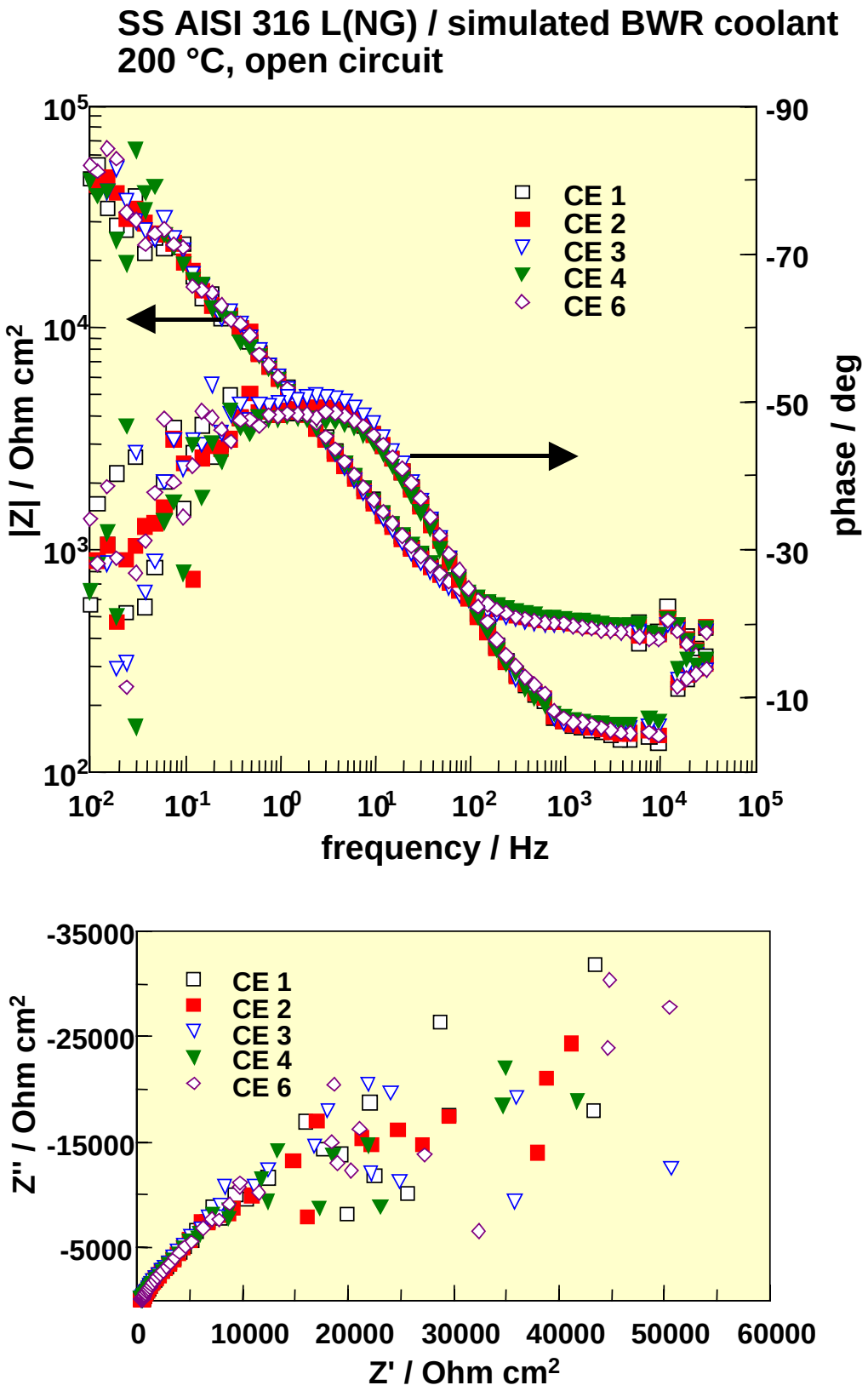

Figure 5. The influence of the location of the counter electrode (see Fig. 4) on the impedance spectrum of SS AISI 316 L(NG) at open circuit in deoxygenated pure water at 200 ℃: a Bode plot presentation (above) and a complex plane presentation (below)

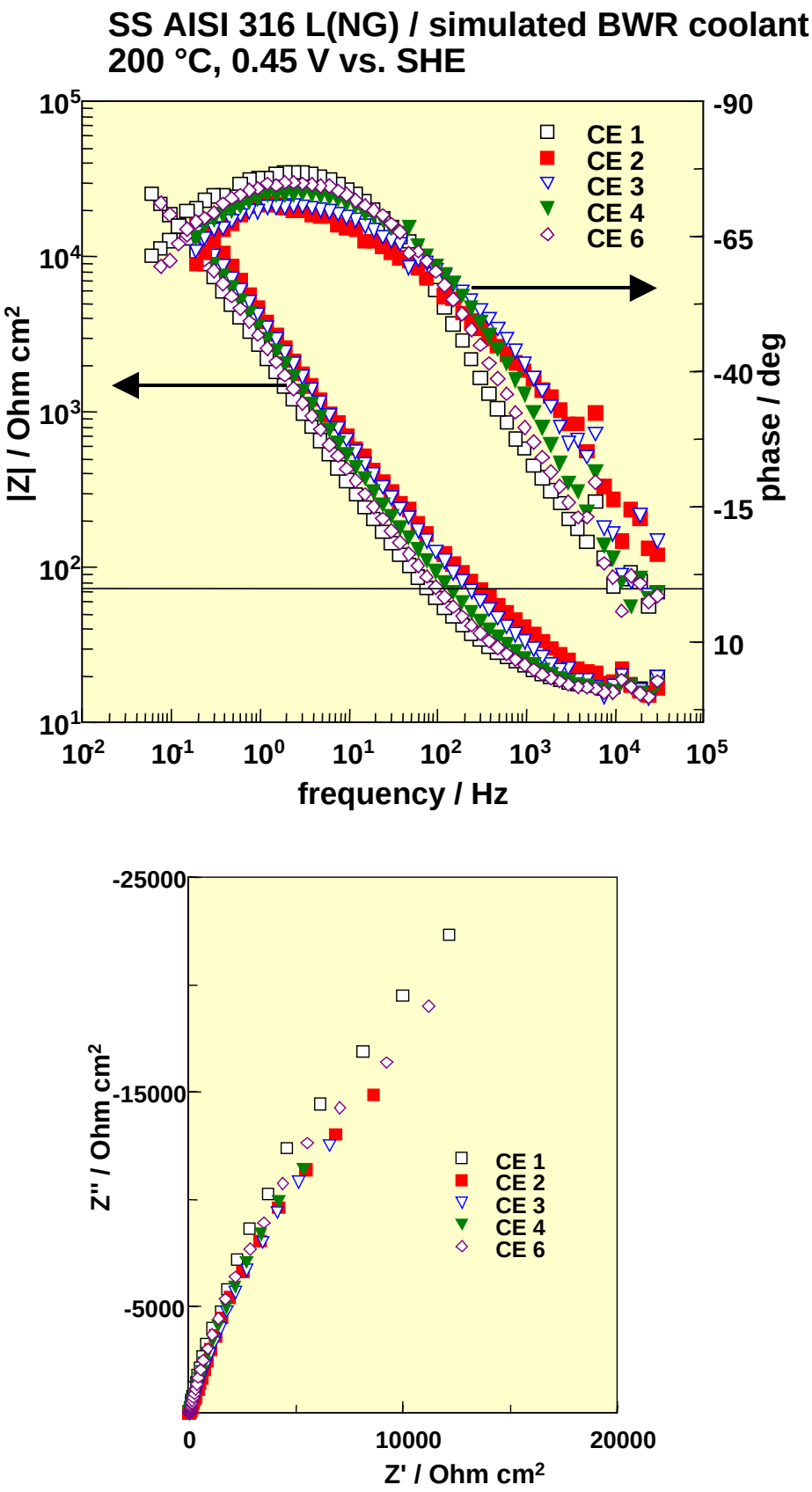

Figure 6. The influence of the location of the counter electrode (see Fig. 4) on the impedance spectrum of SS AISI 316 L(NG) polarised at 0.45 V vs. SHE in deoxygenated pure water at 200 ℃: a Bode plot presentation (above) and a complex plane presentation (below).

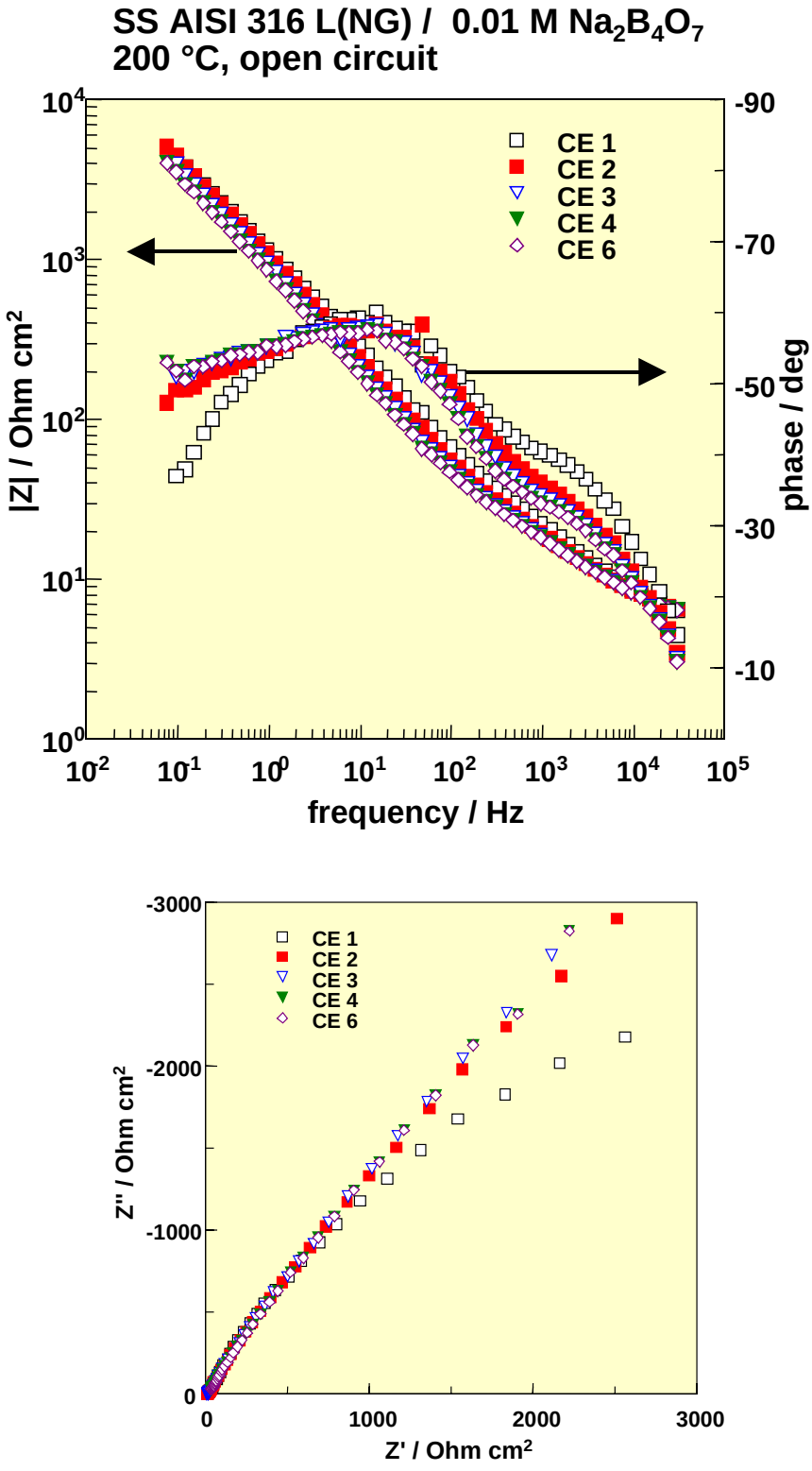

Figure 7. The influence of the location of the counter electrode (see Fig. 4) on the impedance spectrum of SS AISI 316L(NG) at open circuit in deoxygenated 0.01 M $Na_2B_4O_7$ at 200 ℃: a Bode plot presentation (above) and a complex plane presentation (below).

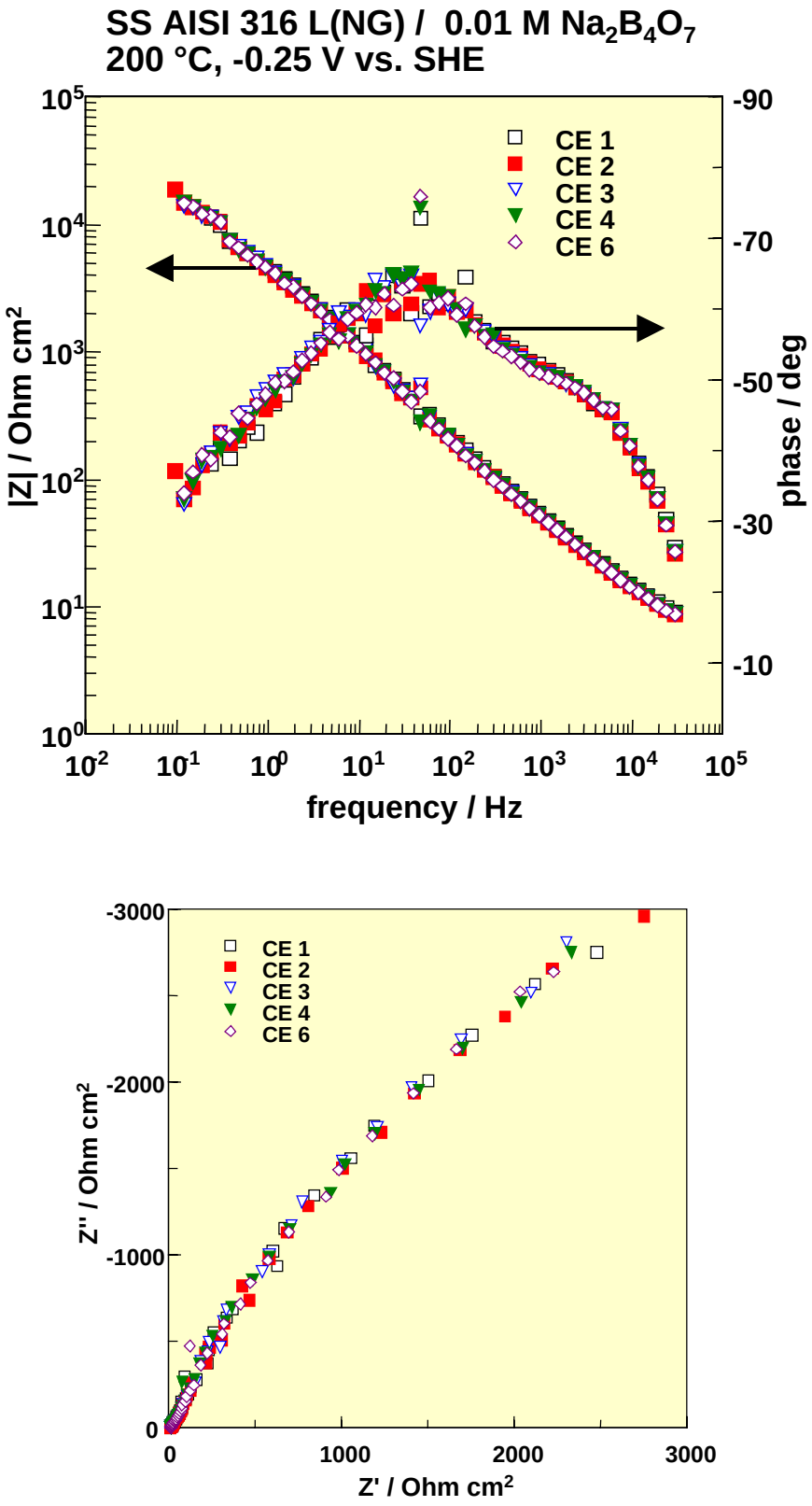

Figure 8. The influence of the location of the counter electrode (see Fig. 4) on the impedance spectrum of SS AISI 316 L(NG) polarised at -0.25 V vs. SHE in deoxygenated 0.01 M $Na_2B_4O_7$ at 200 ℃: a complex plane presentation (above) and a Bode plot presentation (below).

3.3.2 Alternative TLEC configuration: Ir as a counter electrode

Using Ir as a counter electrode makes it possible to reduce the distance of the counter electrode from the working electrode to very low values. This is how relatively high polarisation currents can be passed through the working electrode without exceeding the power output of the potentiostat.

Fig. 9 shows the comparison of impedance spectra for SS AISI 316 L(NG) in simulated BWR coolant measured with the standard TLEC configuration and the alternative configuration. Except for the high-frequency part, the responses are closely similar. The differences at high frequencies are in agreement with the model presented by Chechirlian et al. [10] for the artefacts observed in the impedance response in low-conductivity systems. They have attributed this kind of experimental artefacts to a resistive-capacitive coupling between the electrodes.

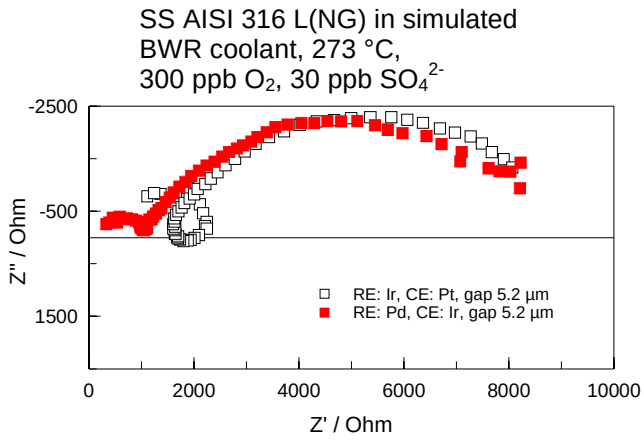

Figure 9. Impedance spectrum of SS AISI 316 L(NG) at open circuit in simulated BWR coolant at 273 °C measured with the standard (the Ir tip as a reference electrode) and with the alternative TLEC configuration (the Ir tip as a counter electrode). Oxygen content 300 ppb.

The results shown in Fig. 10 demonstrate that changing the distance of the reference electrode from the side of the working electrode has almost no or only a minor influence on the impedance response of the alternative TLEC configuration, as far as this distance is much bigger than the gap between the counter and working electrodes. Accordingly, the alternative configuration in the TLEC arrangement is not sensitive to the distance of the reference electrode from the working electrode in a BWR coolant.

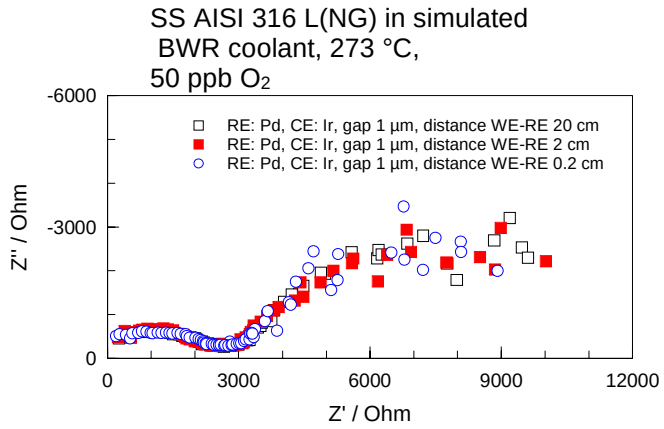

Figure 10. The influence of the distance between the working electrode and a Pd reference electrode on the impedance spectrum of SS AISI 316 L(NG) at open circuit in simulated BWR coolant at 273 ℃. Oxygen content 50 ppb.

The result shown in Fig. 11 demonstrates that the impedance spectrum of SS AISI 316 L(NG) measured in a 10000 ppb SO_4^{2-} solution ($\kappa \cong 0.1$ mScm^{-1}) with the alternative TLEC configuration deviates significantly from that measured using the standard configuration (see Fig. 3). In addition, the spectrum measured with the alternative geometry is distorted, and its shape is greatly dependent on the distance of the gap between the working and the counter electrode. This points to some anomalities due to the experimental arrangement. Accordingly, the results obtained using the alternative configuration cannot be considered correct in this case.

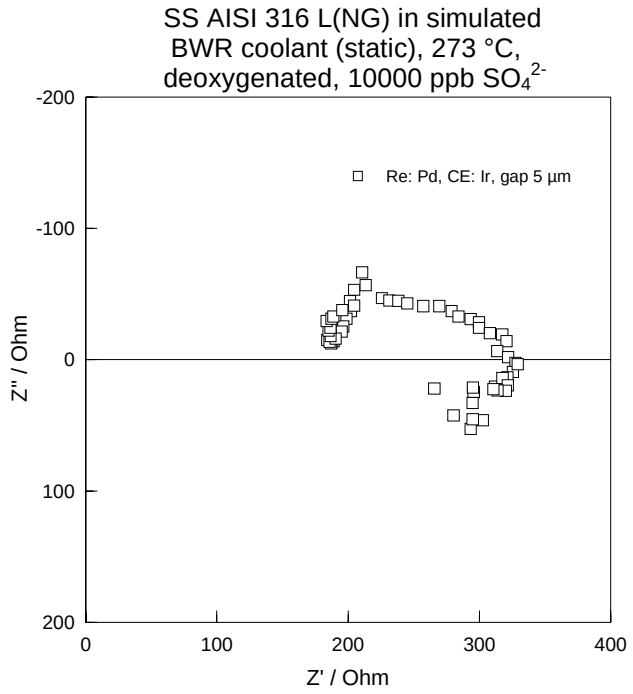

Figure 11. The impedance spectrum of SS AISI 316 L(NG) at open circuit in a deoxygenated solution containing 10000 ppb SO_4^{2-} ions ($\kappa \cong 0.1$ mScm^{-1}) at 273 °C measured with the alternative TLEC configuration, i.e. the Ir tip acts as a counter electrode. E_{corr} = -0.39 V_{SHE}.

3.3.3 An additional possibility to control the potential

Another possible configuration for thin-layer electrochemical measurements is based on the use of a ring-shaped Pt electrode situated around the disc-shaped working electrode (see Fig. 1). The results given in Figs 12 and 13 show that the use of this Pt ring as a reference electrode gives analogous results to those obtained when using the Ir tip as a reference electrode (Fig. 12) and when using a Pd wire at the side of the working electrode (Fig. 13) as a reference electrode. When using the Pt ring as a reference, either the Ir tip or an additional Pt electrode can act as a counter electrode. The results shown in Figs 12–13 indicate that when performing measurements in solutions with a relatively high conductivity the gap between the electrodes should be at least 20 µm. This is necessary to avoid experimental artefacts due to a resistive-capacitive coupling between the electrodes.

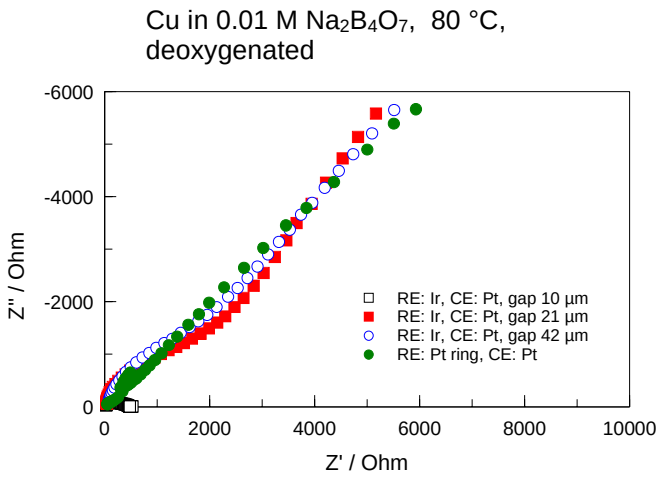

Figure 12. Comparison of the impedance response of Cu in 0.01 M $Na_2B_4O_7$ at 80 °C ($\kappa \cong 3$ mScm^{-1}) when using the Ir tip and when using a Pt ring as a reference electrode. In the former case the effects of different distances between the working and reference electrodes were tested.

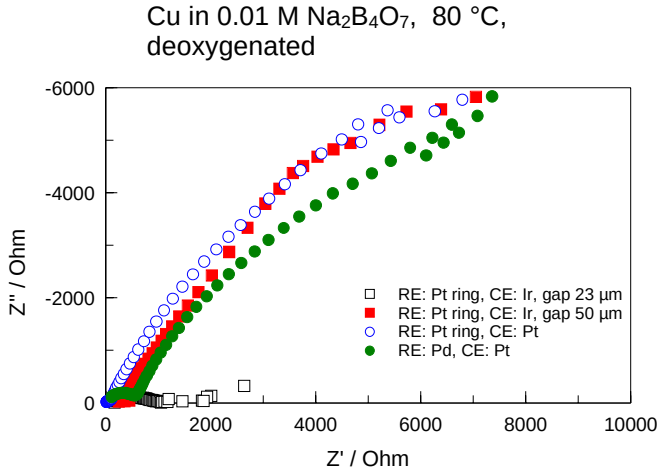

Figure 13. Comparison of the impedance response of Cu in 0.01 M $Na_2B_4O_7$ at 80 °C ($\kappa \cong 3$ mScm^{-1}) when using a Pt ring and when using a Pd wire at the side of the working electrode as a reference electrode. In the former case the effects of different distances between the working and counter electrodes were tested.

3.4 Summary and conclusions

The main conclusions concerning the optimisation of TLEC reported in this work can be summarised as follows:

- The standard TLEC configuration, in which the Ir tip is used as a reference electrode and the counter electrode is situated outside the gap, can be used for electrochemical measurements both in pure water (BWR coolant) and in more conductive solutions. The use of this configuration in aqueous solutions, the conductivity of which corresponds to that of pure BWR water, is probably limited to measurements with low polarisation currents.

- The location of the counter electrode does not have a significant influence on the impedance response of the standard TLEC configuration.

- The distance of the working electrode and the reference electrode in the standard configuration can be varied between 5 and 21 μm.

- The alternative TLEC configuration, in which the Ir tip is used as a counter electrode and the reference electrode is situated outside the gap, is suitable for electrochemical measurements both with small and large polarisation currents in aqueous solutions, the conductivity of which corresponds to that of pure BWR water.

- In solutions with a slightly higher conductivity ($\kappa \cong 100$ μScm^{-1}), the use of the alternative TLEC configuration may result in an anomalous response. Accordingly, the use of the Ir tip as a reference is recommended in these cases.

- Another possible TLEC configuration is obtained when a ring-shaped reference electrode is situated around the working electrode.

4. High temperature wall-jet ring-disc measurements using the CDE arrangement

4.1 Objective

The aim of the work described in this chapter was:

- to verify the operation of a high-temperature wall-jet ring-disc electrode arrangement using pure Cr as a reference material
- to optimise the flow conditions and the construction of the wall-jet ring-disc arrangement
- to investigate the influence of Mo on the transpassive dissolution of Cr from Fe-Cr-Mo alloys.

4.2 Experimental

A high-temperature wall-jet ring-disc electrode is accomplished, when the bulk solution is pumped through the Ir tip perpendicularly onto the working electrode surface in a CDE arrangement (see for instance Fig. 1). The pumping of the bulk solution ensures that representative solution chemistry prevails in the gap between the electrodes during the measurements. By changing the pumping rate of the bulk solution through the Ir tip or the gap width between the working electrode and the Ir tip, it is possible to change significantly the electrolyte flow rate on the working electrode surface. Therefore, this test arrangement can also be conveniently used to study the effects of solution flow rate and novel water chemistries on the electrochemical properties of oxide films. In this work the bulk solution was pumped through the hole in the Ir tip using a high pressure liquid chromatograph (HPLC) pump (Shimadzu LC-10AD VP). To diminish the pulses resulting from the HPLC pump, a pressure accumulator was installed as shown in Fig. 14.

The materials in the high temperature part of system are made of titanium or zirconium to assure that the solution pumped into the gap is not contaminated by any corrosion products that could be released from less passive material surfaces. To detect soluble species released in corrosion reactions, a detector electrode, analogous to the ring electrode in a conventional rotating ring-disk electrode set-up, can be used in the CDE arrangement as shown in Fig. 1. As the corrosion reactions take place on the surface of the disc electrode, the soluble reaction products are transported in controlled hydrodynamic conditions due to pumping onto the ring electrode where they are oxidised or reduced (depending on the ring potential), and the resulting current is

measured. As the potential of the ring electrode is changed, soluble species with different oxidation states can be detected.

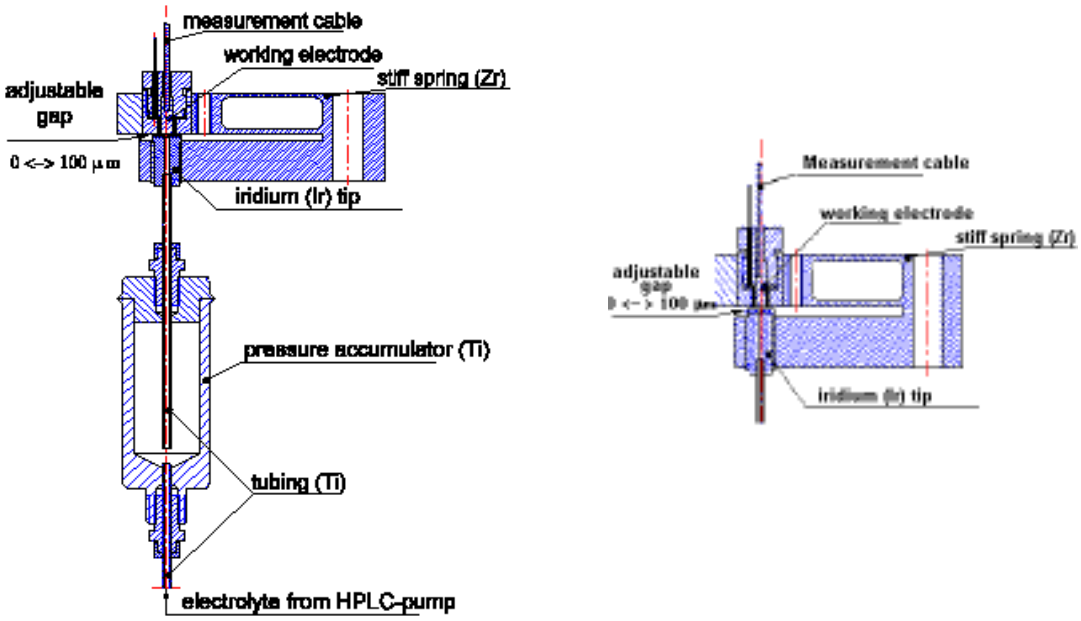

Figure 14. A scheme of the CDE arrangement with the possibility to refresh the solution in the narrow gap between the sample electrode and the Ir tip.

The samples used as disc electrodes in the wall-jet ring-disc experiments were made of 99.7 % Cr, 99.7 % Fe, and Fe-25%Cr, Fe-25%Cr-5%Mo and Fe-25%Cr-10%Mo alloys. The ring electrode was made of pure Pt tube. The electrodes were mechanically polished and rinsed with MILLI-RO® water before the measurements. An external pressure-stabilised Ag/AgCl (0.1 M KCl) electrode, a Pd electrode and the Ir-tip were used as reference electrodes. Prior to all the experiments, the disc electrode was polarised cathodically for 240 seconds.

These measurements were performed in a static autoclave at 200 °C in a 0.1 M $Na_2B_4O_7$ solution. Prior to tests the solution was deoxygenated by using 99.999% nitrogen bubbling.

An Autolab PGSTAT20 equipment controlled by Autolab GPES-software was used in the experiments. The distance between the electrodes in the arrangement was controlled by means of a CER equipment supplied by Cormet Ltd.

4.3 Results and discussion

4.3.1 Wall-jet ring-disc measurements to study the effects of electrolyte flow rate and distance between the working electrode and the Ir tip

The aim of the work discussed in chapter 4.3.1 was to verify the operation of the high-temperature wall-jet ring-disc arrangement using Cr as a reference material at the disc, as well as to study the influence of the flow rate and the distance between the working electrode and the Ir tip on the response of the system.

Our previous measurements have shown that the wall-jet ring-disc arrangement allows a qualitative detection of the dissolution of Cr(VI) from a Cr disc electrode at different temperatures. Fig. 15 shows the measurement result of such a typical test run at 200 ^{o}C. The current at the Cr disc increases clearly at E > 0 V_{SHE}. This increase has been related to the oxidation of Cr (III) to Cr (VI). Simultaneously, a negative current at the Pt ring polarised at -0.550 V_{SHE} is observed. This negative ring current is due to the reduction of Cr(VI) released from the disc as a result of the transpassive dissolution of Cr. During the backward sweep, the current of the ring electrode returns rapidly close to the background current level, which was measured in the beginning of the sweep.

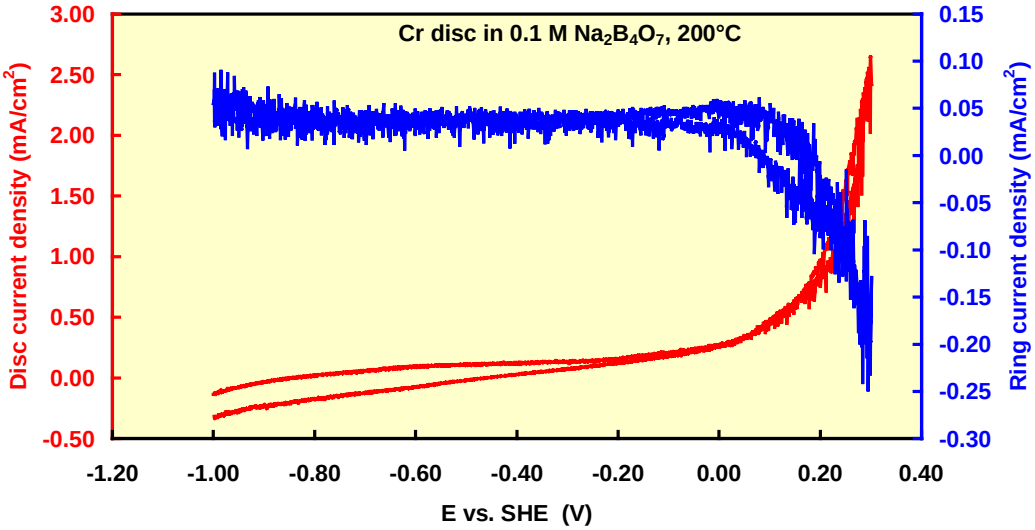

Figure 15. Reduction of soluble Cr(VI) species on the ring electrode in a 0.1 M $Na_2B_4O_7$ solution at 200 °C measured using a high-temperature wall-jet ring-disc arrangement. Sweep rate was 2 mVs^{-1}, ring potential was kept at -0.550 V_{SHE} and volume flow rate 6 $mlmin^{-1}$ on to the disc electrode. Gap = 37 µm.

The current noise level was successfully decreased by replacing all teflon parts in the design by oxidised Zr and ceramic ZrO_2 parts. Particularly at high temperatures, teflon parts in the older design deformed, and therefore, the accuracy of controlling the distance between the working electrode and the Ir tip was lost. One set of results obtained using the new ceramic parts is shown in Fig. 16.

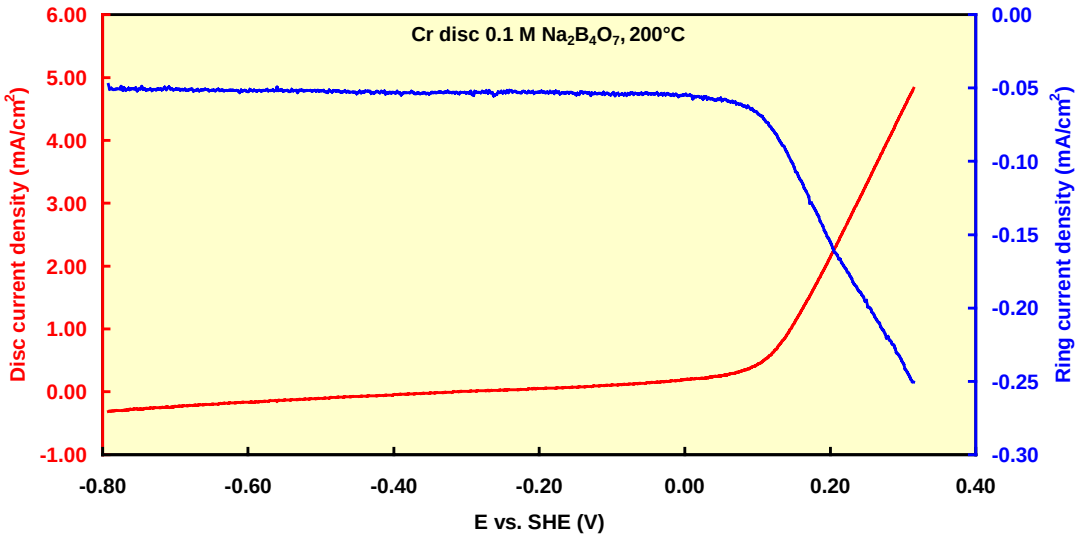

Figure 16. Reduction of soluble Cr(VI) species on the ring electrode in a 0.1 M $Na_2B_4O_7$ solution at 200 °C measured using an up-dated high-temperature wall-jet ring-disc arrangement. Sweep rate was 2 mVs^{-1}, ring potential was kept at -0.550 V_{SHE} and volume flow rate 6 $mlmin^{-1}$ on to the disc electrode. Gap = 37 µm.

The Pourbaix diagram for chromium, calculated by Beverskog et al., is shown in Fig. 17 [11]. The potential-pH_T value, at which the release of soluble Cr(VI) from the Cr disc is experimentally observed at 200 ^oC, is shown in the diagram. This experimental point is clearly in the potential-pH_T region where Cr(III) is expected to be oxidised to Cr(VI).

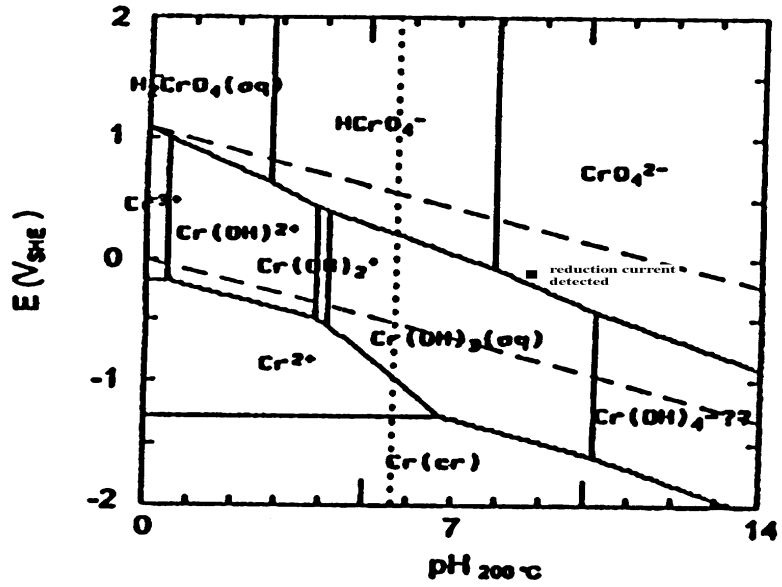

Figure 17. Pourbaix diagram for chromium at 200 °C [Cr(aq)]$_{tot}$ = 10^{-8} m] [11].

The distance between the working electrode and the Ir tip has a significant effect on the measurement results as shown in Fig. 18: An increase of the gap width from 10 µm to 37 µm causes the chromium dissolution to start at somewhat lower potentials, which is still in the stability region of Cr(VI) calculated by Beverskog et al. (see Fig. 17).

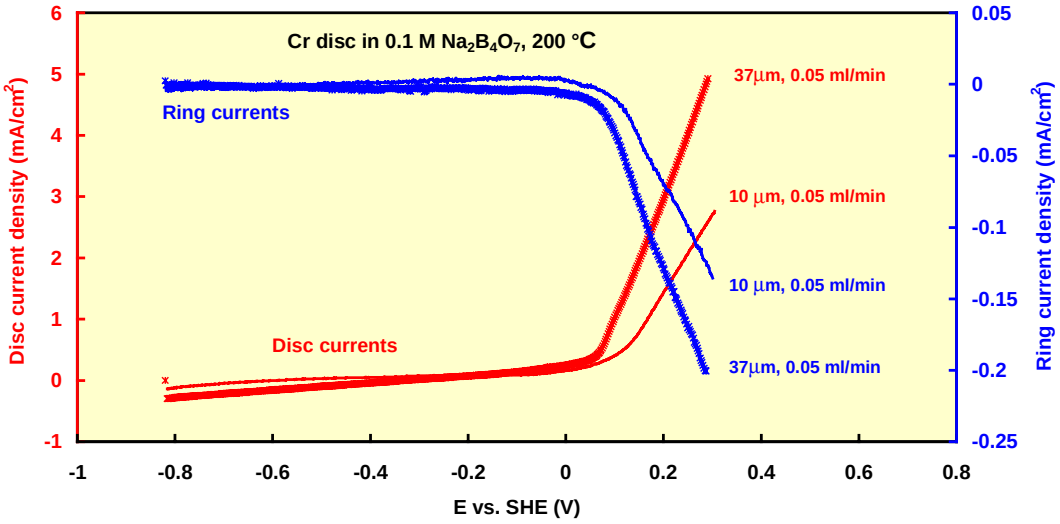

Figure 18. Effect of the distance between the working electrode and the Ir tip on the wall-jet ring-disc detection of soluble Cr(VI) species on the ring electrode in a 0.1 M $Na_2B_4O_7$ *solution at 200 °C. Sweep rate was 2 mVs^{-1}, ring potential was kept at -0.550* V_{SHE} *.*

The effect of flow rate on the measured current densities was not significant in chromium studies. Having a constant distance of 37 μm between the working electrode and the Ir tip, the volume flow rate of the electrolyte through the Ir tip was increased from 0.01 ml/min to 5 ml/min. This resulted in slightly higher anodic current densities at the disc at high potentials and in slightly higher cathodic current densities at the ring. In addition, the ring current exhibited a maximum at potentials close to 0.1 V_{SHE}, when the volume flow rate was increased to 5 ml/min, as shown in Fig. 19.

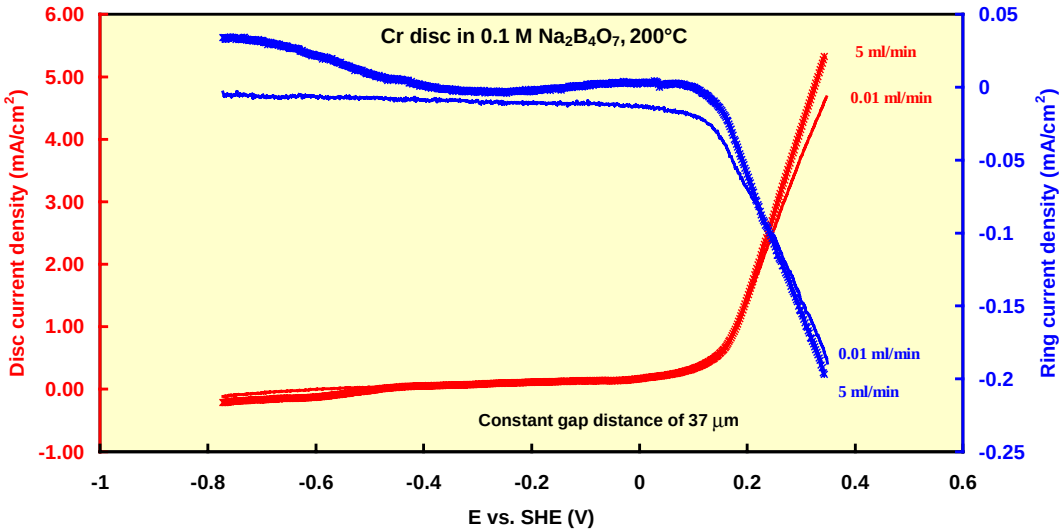

Figure 19. Effect of flow rate on the wall-jet ring-disc detection of soluble Cr(VI) species on the ring electrode in a 0.1 M $Na_2B_4O_7$ solution at 200 °C. Sweep rate was 2 mVs^{-1}, ring potential was kept at -0.550 V_{SHE} . Gap = 37 μm.

However, the flow rate was found to have a significant effect on the electrochemical response of the Fe-Cr-Mo alloys, an example of which is given in Fig. 20. The same sample was used in both of the measurements shown in the figure. After the first sweep, the autoclave was cooled down and the sample surface was polished. Therefore, differences in surface roughness or composition were likely to be minimal. Between the tests the autoclave was rinsed twice with high purity water, and a fresh solution was placed into the autoclave.

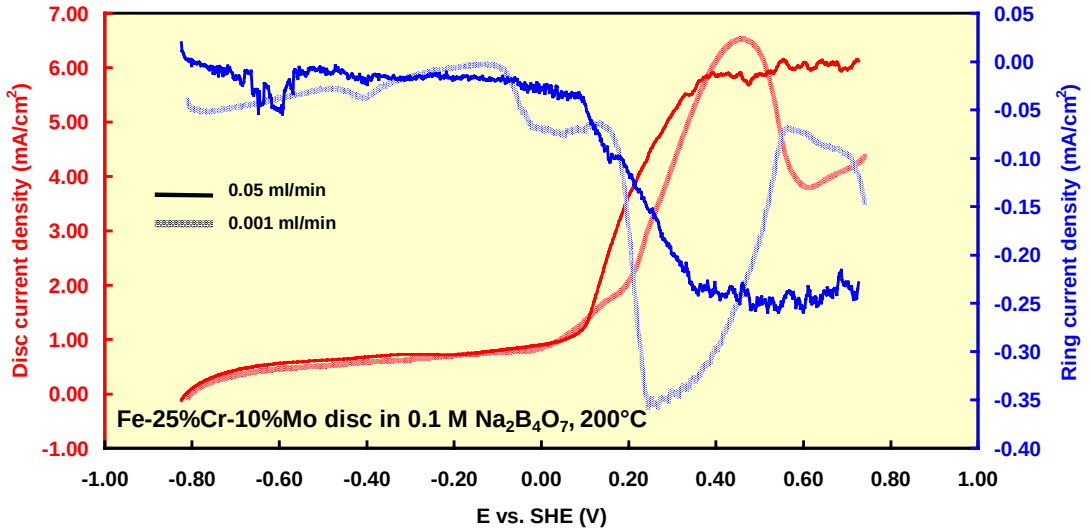

Figure 20. Linear positive-going voltammograms for Fe-25%Cr-10%Mo in 0.1 M $Na_2B_4O_7$. Sweep rate 2 mV/s. The gap between working electrode and Ir tip was kept constant 37μm. Electrolyte was pumped into the gap using two different volume flow rates.

On the basis of these observations we considered it necessary to look more carefully into the factors that affect the flow conditions in the wall-jet ring-disc arrangement.

4.3.2 Estimation of the flow conditions in the wall-jet ring-disc electrode arrangement

The aim of the work described in this chapter was to find out in which flow conditions the disc electrode surface in a wall-jet ring-disc arrangement can be considered uniform with respect to oxide film properties.

As indicated in the previous chapter, the Fe-25%Cr-10%Mo sample at high potentials showed a different behaviour in the wall-jet ring-disc experiments at the volume flow rate of 0.001 ml/min from those at 0.05 ml/min. When the disc electrode surfaces were examined microscopically, the influence of different flow conditions became obvious. The lower volume flow rate led to the formation of an even oxide film whereas the higher volume flow rate led to the formation of a ring-shaped pattern on the electrode surface, as shown in Fig. 21. The lighter colour of the ring-shaped pattern refers to a smaller thickness of the film at this pattern than in the other parts of the surface. On the other hand, the whole surface of the sample, which had been exposed to the lower volume flow rate, exhibited a uniform colour and thus an even thickness of the oxide film. The overall colour of this latter sample was lighter and thus the film thickness was

lower than that of the former sample. This observation, however, is not relevant in this context, because it can be attributed to the shorter exposure time to the high temperature electrolyte and is thus not directly connected with the flow conditions.

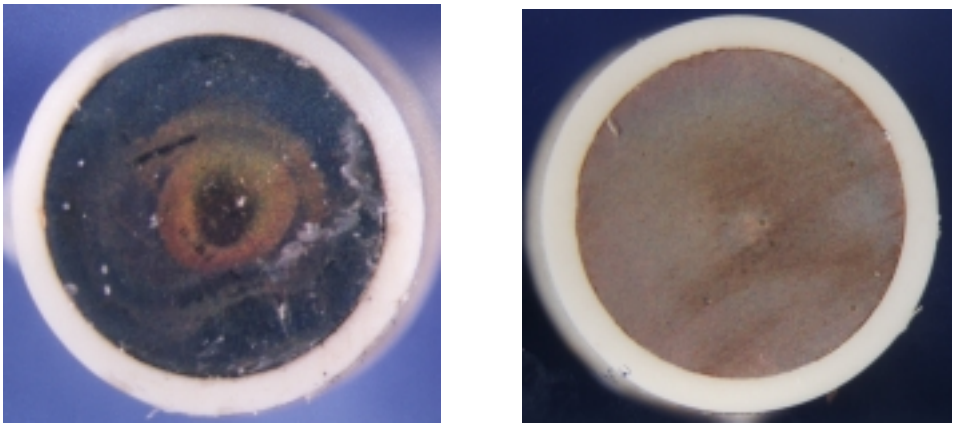

a) b)

Figure 21. The disc electrode surface after two tests: (a) volume flow rate 0.05 ml/min and (b) volume flow rate 0.001 ml/min. The diameter of the disc electrode was 5 mm.

Possible reasons for the phenomenon shown in Fig. 21 may be water-induced mechanical wear, a turbulent flow within the narrow gap or the transport of chemical species to or from the disc electrode surface.

To investigate the possibility of turbulent flow conditions, the flow distribution inside the wall-jet ring-disc electrode was calculated using the FLUENT-programme. The calculation was carried out for the 0.5 mm flow-through hole in the Ir electrode and for the 37 μm gap between the Ir and working electrodes (see Figs 14, 22–24). Calculations were performed using two different volume flow rates, namely 0.05ml/min and 0.001 ml/min. The Reynolds number proved to be so small that the flow is laminar in all parts of the wall-jet ring-disc electrode, as can be seen also in the Fig. 22.

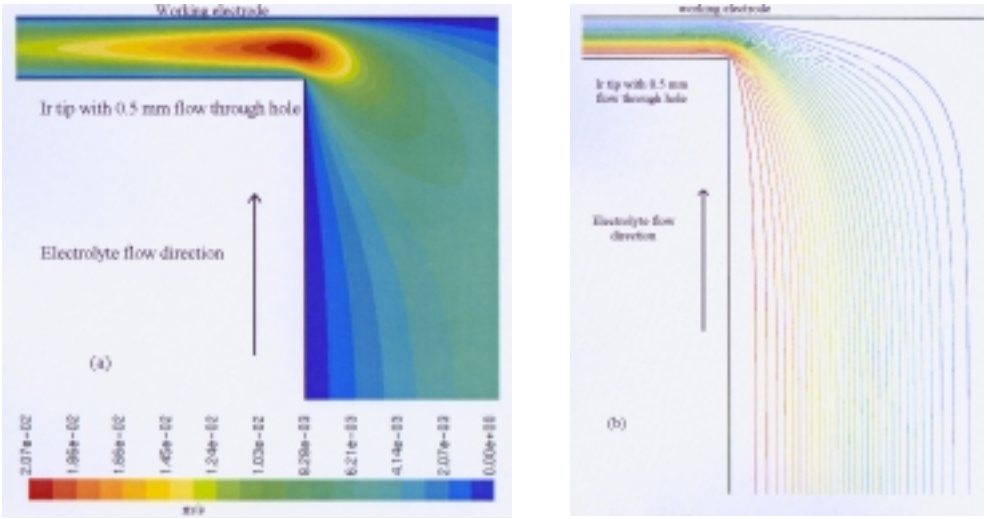

Figure 22. Flow rate (a) and the flow patterns (b) in the wall-jet ring-disc electrode. 0.05 ml/min electrolyte was pumped using a HPLC-pump.

The maximum electrolyte flow rate is roughly 2 cm/s (volume flow rate 0.05 ml/min) giving a Reynolds number which is close to one. The flow patterns in the wall-jet ring-disc electrode are even, and no evidence of turbulent flow can be seen. Therefore, turbulence cannot explain the observed pattern on the disc electrode surface.

As commented above, one possible explanation to the observed uneven oxide film could be the influence of flow on the transport of chemical species to or from the disc electrode surface. These phenomena are influenced by the axial velocity (the flow component which is towards the disc electrode surface) and the wall shear stress. Figs. 23a and 23b show the axial velocities on the disc electrode, calculated using the FLUENT-programme. Fig 23a shows an area on the surface where the electrolyte flow is towards electrode (white spot). Similarly, in Fig 23b (volume flow rate 0.05 ml/min) there is an area on the surface in which the flow is towards the electrode surface approximately in the same position where the thinner oxide film was observed. A similar phenomenon is not observed with the lower volume flow rate. Although an axial velocity component was observed to be positive with the higher volume flow rate, its absolute magnitude is relatively small.

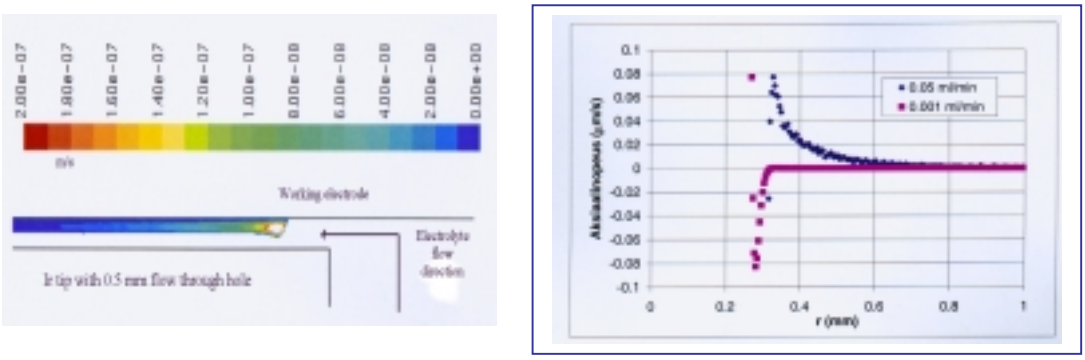

a) b)

Figure 23. a) Axial velocity (component which is vertical to the working electrode surface) on the surface of the working electrode (within the 37 μm gap) when the pumping rate was 0.05 ml/min; b) Axial velocity as a function of the distance on the working electrode surface. 0 mm is the middle point of the water jet impacting the electrode surface (actually the middle point of the working electrode).

The wall shear stress values estimated using the FLUENT-programme are shown in Figs. 24 a) and b). The shapes of the curves are similar for both volume flow rates, but the actual values are clearly higher when the electrolyte was pumped using the 0.05 ml/min rate. The maximum value of the wall shear stress is almost in the same position where the oxide film starts to change colour. The maximum wall shear stress values with the lower pumping rate (0.001ml/min) are in the same range as those, which were calculated for the higher volume flow rate at the distance of 1.6 mm from the centre of the disc electrode.

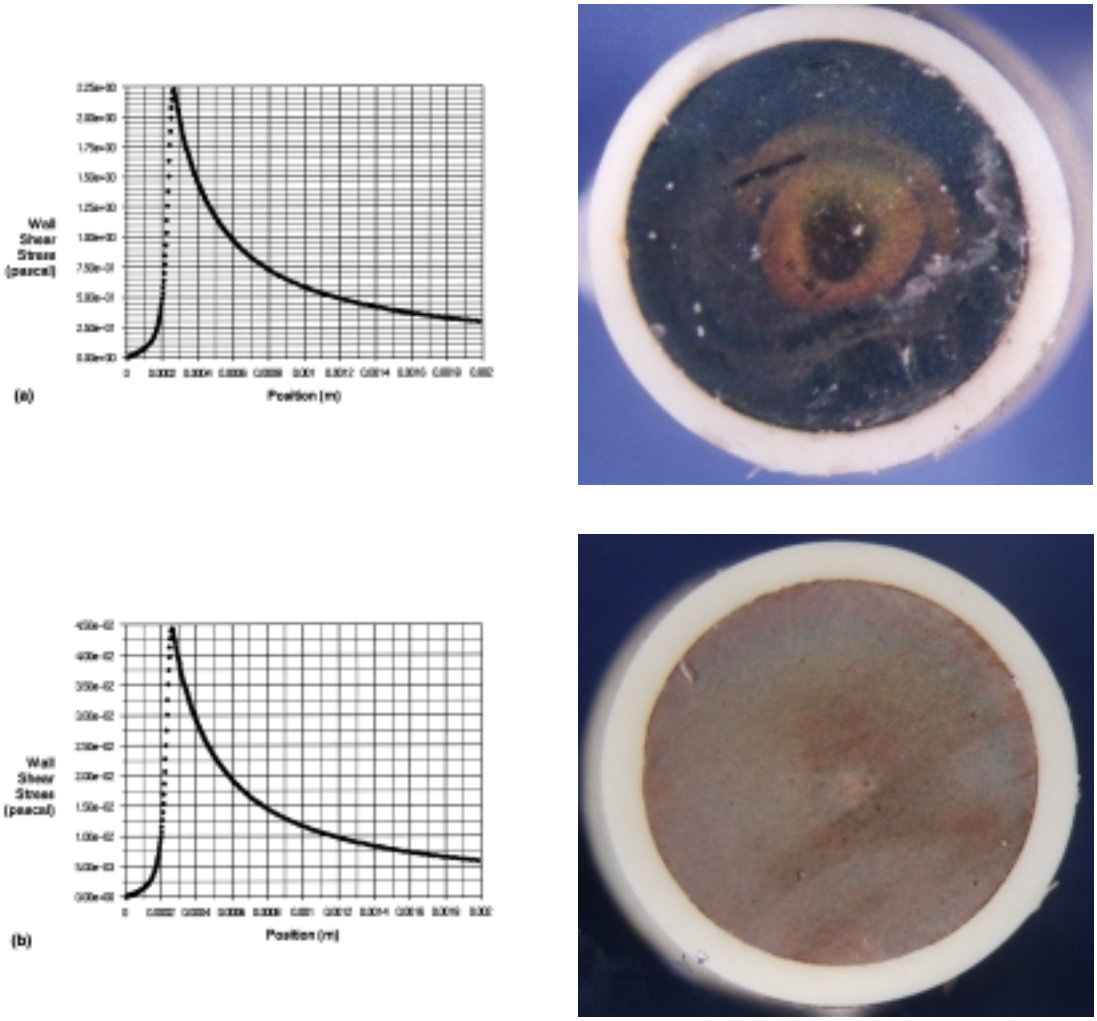

Figure 24. Wall shear stress on the disc electrode surface as a function of distance from the middle point of the disc electrode using two different volume flow rates: (a) 0.05 ml/min and (b) 0.001 ml/min.

These observations show that the volume flow rate and electrode configuration need to be optimised in order to maintain uniform conditions over the disc electrode surface. To decrease the electrolyte flow rate in the wall-jet ring-disc arrangement it is necessary to re-design the stiff spring in such a way that a larger movement of the electrodes becomes possible. Furthermore, if the diameter of the impecting electrolyte jet is larger than the disc electrode surface, the flow rates obtained would be in low enough a range to achieve acceptable uniform flow conditions.

The use of the system to study the effects of high flow rates (in the range 0.1–10 m/s) and/or turbulent flow conditions needs further optimisation of the electrode configuration.

4.3.3 Wall-jet ring-disc measurements to estimate the effect of Mo on the transpassive dissolution of Cr from Fe-Cr-Mo alloys

The aim of the preliminary measurements described in this chapter was to find out how molybdenum influences the transpassive dissolution of Cr from Fe-Cr-Mo alloys at high temperatures. Alloying steels with chromium and molybdenum has been used to reduce their susceptibility to general and localised corrosion.. However, doing so the steels are more prone to general corrosion in highly oxidising operational environments due to enhanced transpassive dissolution processes.

In order to verify the representativenes of the electrochemical measurements with the wall-jet ring-disc arrangement, voltammograms for the Fe-Cr-Mo alloys were first measured using stationary samples exposed freely to 0.1 M $Na_2B_4O_7$ at 200 ^oC in a static autoclave. The reproducibility of these voltammograms was extremely good. This was probably due to the fact that in each measurement static conditions existed in the autoclave. One set of these results is shown in Fig. 25. The results clearly indicate that transpassive dissolution starts at the same potential, which was observed for the pure Cr as shown in the Figs 15 and 16. Unlike in the case of pure chromium, a clear secondary passivation is observed for all the alloys. This may be due to the fact that as the film gets depleted in Cr due to the transpassive dissolution, an iron-rich secondary oxide film is formed on the alloy. Furthermore, the transpassive oxidation currents in stagnant flow conditions are the higher, the higher is the molybdenum content in the alloy.

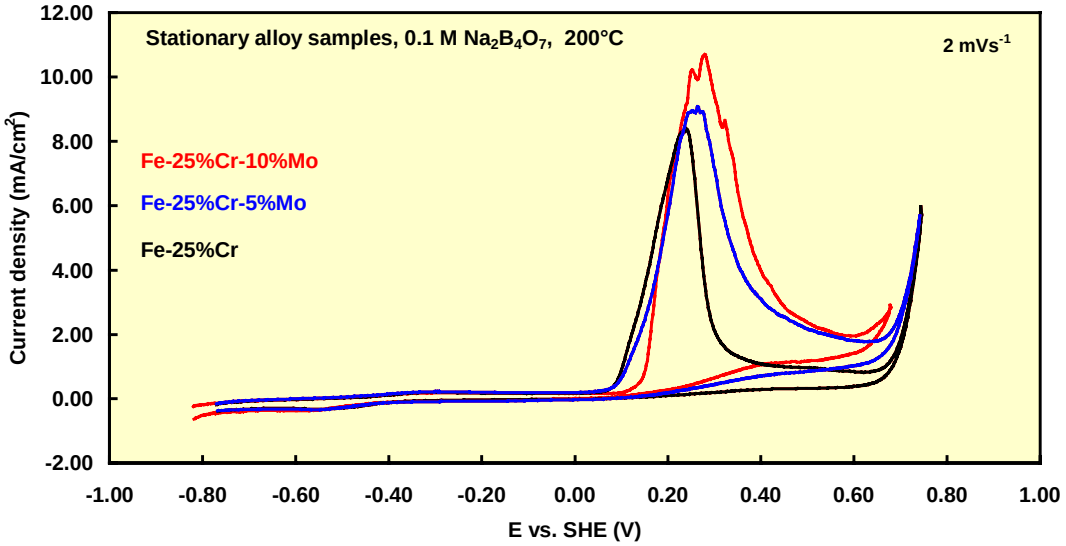

Figure 25. Linear sweep voltammograms for stationary samples of Fe-25%Cr, Fe-25%Cr-5%Mo and Fe-25%Cr-10%Mo at 200 °C in 0.1 M $Na_2B_4O_7$ in a static autoclave. Sweep rate 2 mV/s.

The transpassive dissolution of Cr due to oxidation of Cr(III) to Cr(VI) starts in the same potential range (E > 0 V_{SHE}) for the samples in the wall-jet ring-disc arrangement (see Fig. 26) as for the stationary samples (Fig. 25). However, the results obtained with the wall-jet ring-disc arrangement show two significant differences when compared with the results obtained with the stationary samples. First, the higher the Mo content of the alloy, the lower transpassive oxidation currents were measured with the wall-jet ring-disc arrangement, while an opposite behaviour was found with the stationary samples. Secondly, the secondary passivation is much less pronounced for all the studied alloys when using the wall-jet ring-disc arrangement.

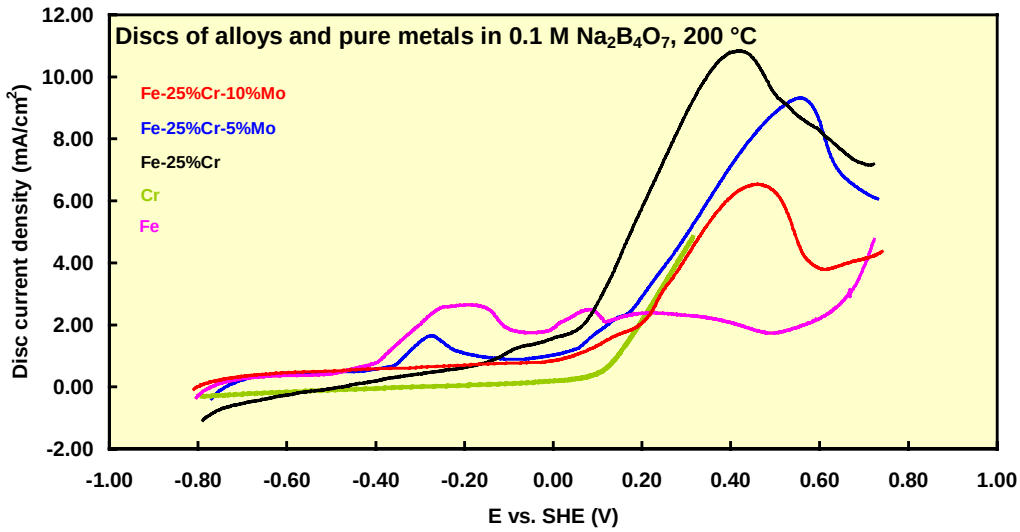

Figure 26. Linear positive-going potential sweeps for Fe, Cr, Fe-25%Cr, Fe-25%Cr-5%Mo and Fe-25%Cr-10%Mo in a wall-jet ring-disc arrangement in 0.1 M $Na_2B_4O_7$. Sweep rate 2 mV/s. The gap between working electrode and Ir tip was kept constant at 37 μm. Electrolyte was pumped at the rate which allowed us to observe the start of the secondary passivation. The curves have not been corrected for IR drop, because it was estimated to be insignificant (less than 20 mV).

During the potential sweeps of the disc electrodes shown in Fig. 26, the Pt ring electrode in the CDE arrangement was polarised at -0.550 V_{SHE} to detect oxidised species from the flowing electrolyte. One set of results is shown in Fig. 27. Simultaneously with the increase of the disc current due to transpassive oxidation of Cr at E > 0 V_{SHE}, a negative ring current is observed. This negative ring current can be attributed to the reduction of Cr(VI) at the ring. Thus this result supports the idea of transpassive dissolution of chromium (VI) from the oxide film. Similar measurements with Fe do not produce any significant reduction peaks at the ring, and thus the measured negative ring currents observed for the alloys can be related solely to the presence of Cr. The magnitudes of the ring currents seem to support the idea that the

higher the molybdenum content, the higher the extent of transpassive dissolution of chromium from the alloy. The opposite trend in the disc curves measured in a flowing electrolyte (see Fig. 26) shows that the addition of Mo results in a smaller overall oxidation rate, although a higher amount of soluble products are released in the presence of Mo.

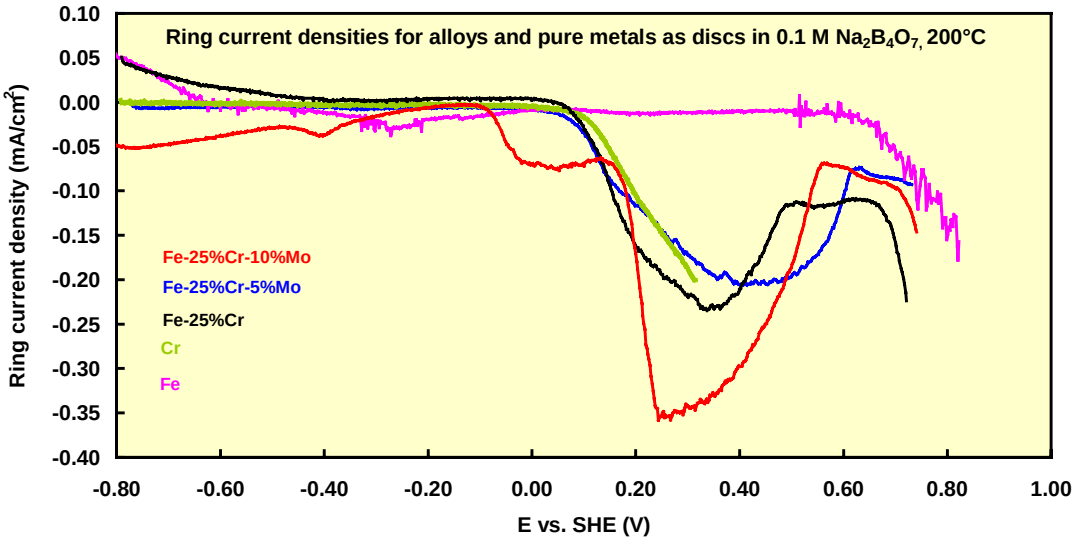

Figure 27. Reduction of soluble species on the ring electrode in a 0.1 M $Na_2B_4O_7$ solution at 200 °C measured using the wall-jet ring-disc arrangement. Sweep rate was 2 mVs^{-1}; ring potential was kept at -0.550 V_{SHE} .

Fig. 28 shows the disc and ring currents during a negative-going potential sweep for a Fe electrode. The potential of the Pt ring electrode was kept at +0.300 V_{SHE}, at which potential divalent iron is oxidised to trivalent iron. During the reduction of the formed oxide film on pure Fe, a two-stage release of divalent iron from the oxide film was observed. This observation can be ascribed to the solid state transformation of the passive film into a lower-valent oxide film and a subsequent reductive dissolution step. A similar release of divalent iron has been postulated from oxide films formed on Fe at room temperature measurements [9 and refs. therein].

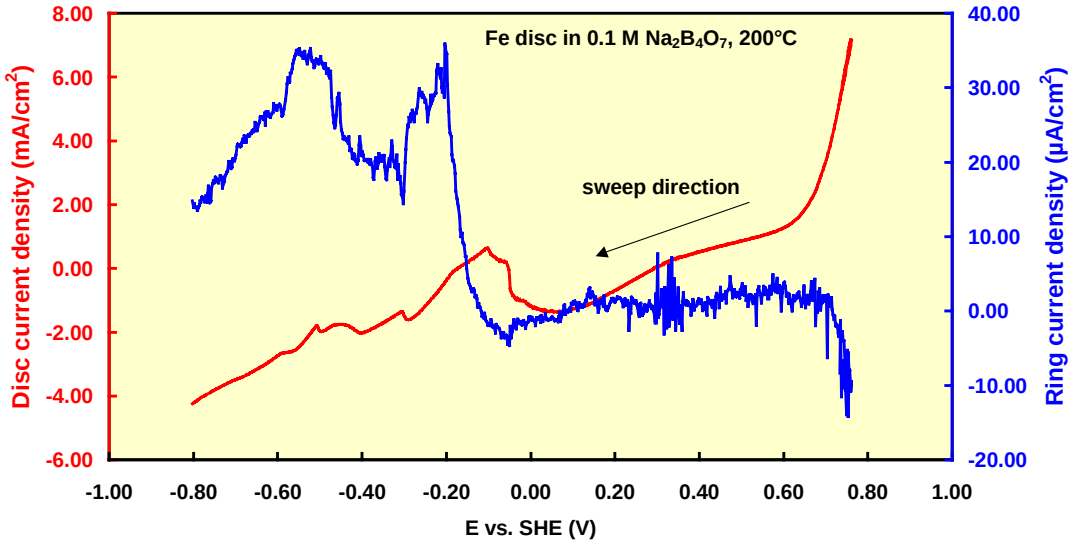

Figure 28. Detection of soluble Fe(II) species on the ring electrode in a 0.1 M $Na_2B_4O_7$ solution at 200 °C measured using the wall-jet ring-disc arrangement. Sweep rate was 2 mVs^{-1}, ring potential was kept at +0.300 V_{SHE} .

4.4 Summary and conclusions

The main conclusions concerning the wall-jet ring-disc arrangement can be summarised as follows:

- The transpassive dissolution of Cr from pure Cr, Fe-Cr and Fe-Cr-Mo alloys can be detected at elevated temperatures (up to 288 ^{o}C) by using the wall-jet ring-disc electrode arrangement.

- The higher the Mo content in the alloy, the higher is the transpassive dissolution of Cr from the alloy.

- The new design of the wall-jet ring-disc arrangement with ceramic parts replacing PTFE gives more stable results.

- To improve the quantitativeness of the results, further optimisation of the flow conditions and electrode configuration is needed.

5. Development of the bellows-driven CDE arrangement

5.1 Objective

The primary goal of the work described in this chapter was to design and test a pneumatically-powered bellows-driven system for CDE measurements in high-temperature water. One of the key requirements of the design was to be able to use several bellows-driven CDE arrangements simultaneously in an autoclave or at a power plant. The design should also make it possible to conduct CDE experiments in a test environment without moving parts through the pressure boundary.

Different types of CDE measurements have different requirements for the accuracy of the distance control. The contact electric resistance (CER) and contact electric impedance (CEI) measurements set the most stringent requirements. In CER measurements performed with a step motor driven system, the achievable accuracy in electrode distance control is $2*10^{-9}$ m, while that used in practice is typically $2*10^{-7}$ m (0.2 μm). Based on this experience, the goal for the accuracy in electrode distance control was set at 0.2 μm.

5.2 Experimental

The preliminary tests were performed in a static autoclave containing high purity water at 288 ^{o}C. The working electrodes used in these tests were made of SS AISI 316 L(NG). Later experiments with the bellows-driven CDE arrangements were performed in a nitrogen/oxygen gas environment at room temperature, using pure nickel as the electrode material.

The main parts of the bellows-driven CDE arrangement are presented in Fig. 29. The system consists of pneumatically powered bellows, springs, electrodes and a servo-controlled pressure adjusting loop.

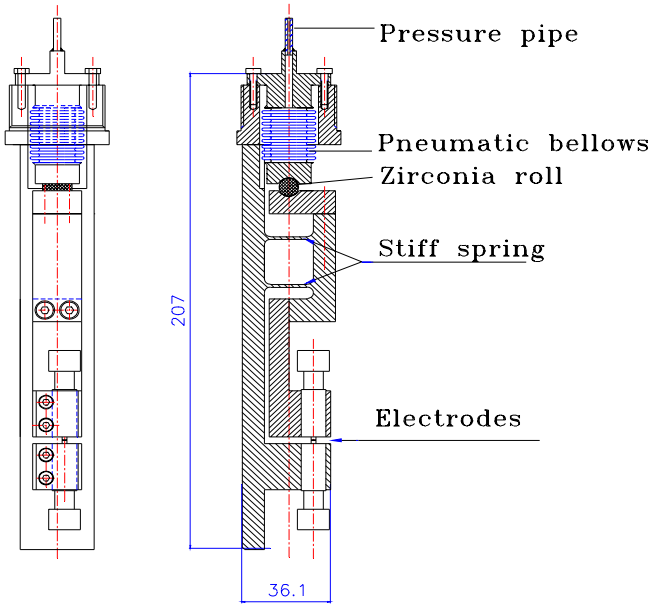

Figure 29. Prototype of the bellows-driven CDE arrangement.

The servo-controlled pressure-adjusting loop which is used to move the tips is presented in Fig. 30. It consists of four pressure areas, namely (A), (B), (C) and (D). The gas flow needed for the servo valve (6) is provided by the high-pressure compressor (1). With this fully automatic compressor an operational pressure level (20 MPa) of the gas is achieved. The pressure variation within the pressure area (A) is from 17.5 to 20 MPa during the test.

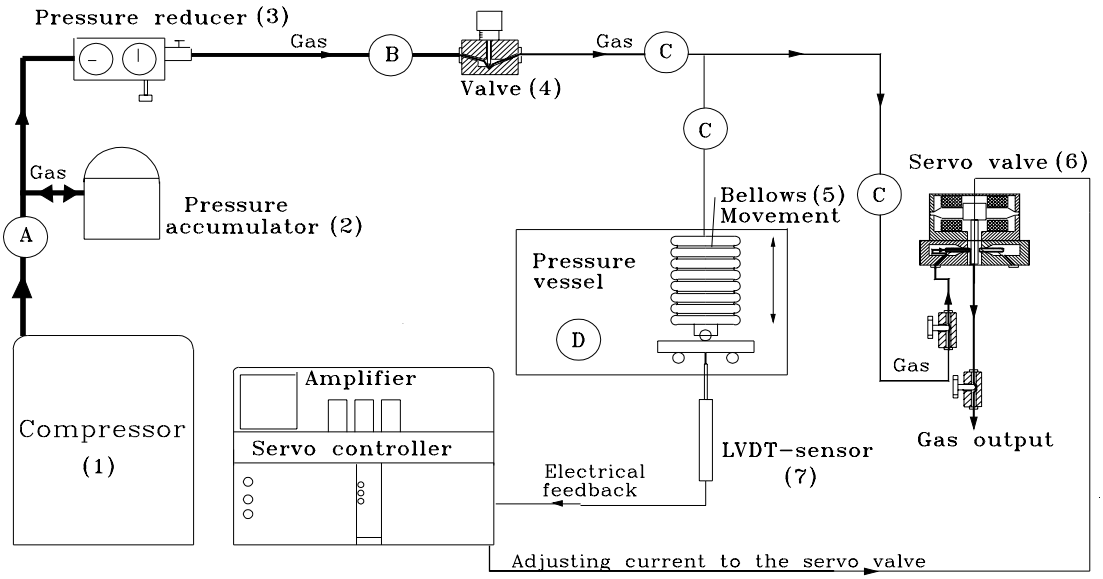

Figure 30. Operating principle of the pneumatic servo-controlled arrangement.

From the pressure accumulator (2) the gas is led to the pressure reducer (3) and further through the manually-controlled valve (4). The pressure adjusted for the area (B) depends on the pressure of the environment in which measurements are performed. The gas is directed from the manually-controlled valve (4) to the bellows (5) and to the servo valve (6) from which the gas flow is let out from the system. With the pressure reducer (3) and the manually-controlled valve (4) together with a suitable initial pressure level, tests under different kind of environmental pressures can be performed.

Adjustment of the bellows pressure (5) and the pressure in area (C) is based on a continuous gas flow through the manually-controlled valve (4) and the servo valve (6). With this kind of pressure area loop, a two-way pressure adjusting system can be created. The servo valve (6) can be opened or throttled for the adjustment of gas flow until the desired pressure level of the bellows (5) is achieved. Throttling will increase the bellows pressure and opening will decrease it.

The generated load is directly proportional to the bellows (5) pressure in pressure area (C). The displacement of the bellows can be determined with a linear variable distance transducer (LVDT) -sensor (7). As an option, it is also possible to control the displacement of the bellows with this LVDT-sensor (7), which gives a feedback signal to the servo controller. The servo controller compares this feedback signal to a pre-set base signal. If the two signals differ, the servo valve can throttle or open for adjustment of gas flow until the feedback and the pre-set base signals become equal. Preliminary tests with the bellows-driven CDE arrangement [8] were performed at room temperature under displacement control using the signal from a LVDT-sensor. The accuracy by which the distance between the electrodes could be controlled was ± 0.1 μm, which appeared accurate enough for CDE measurements. The distance between the electrodes depended on the bellows pressure according the following equation:

$$\beta = \frac{\Delta d}{\Delta p} = 0.1 \ \frac{mm}{MPa} \qquad (1)$$

At room temperature the noise level of the LVDT-sensor was ± 0.05 μm. However, in high temperature water the noise level was measured to be significantly higher (± 0.3 μm). Thus the accuracy of the LVDT-sensor was less than what was required for a successful CDE measurement. This led us to the further development of the system. The results of this development are described in the next chapter.

5.3 Results and discussion

5.3.1 The bellows-driven CDE arrangement using pressure feedback control

The tests at high temperature were performed under pressure feedback control because of the insufficient accuracy of the tests under displacement control. The accuracy by which the distance between the electrodes could be controlled was measured to be better than ± 0.35 μm, as shown in Fig. 31. In addition, it was observed that the position of the electrodes can be best controlled when the pressure of the bellows and the environment were almost equal.

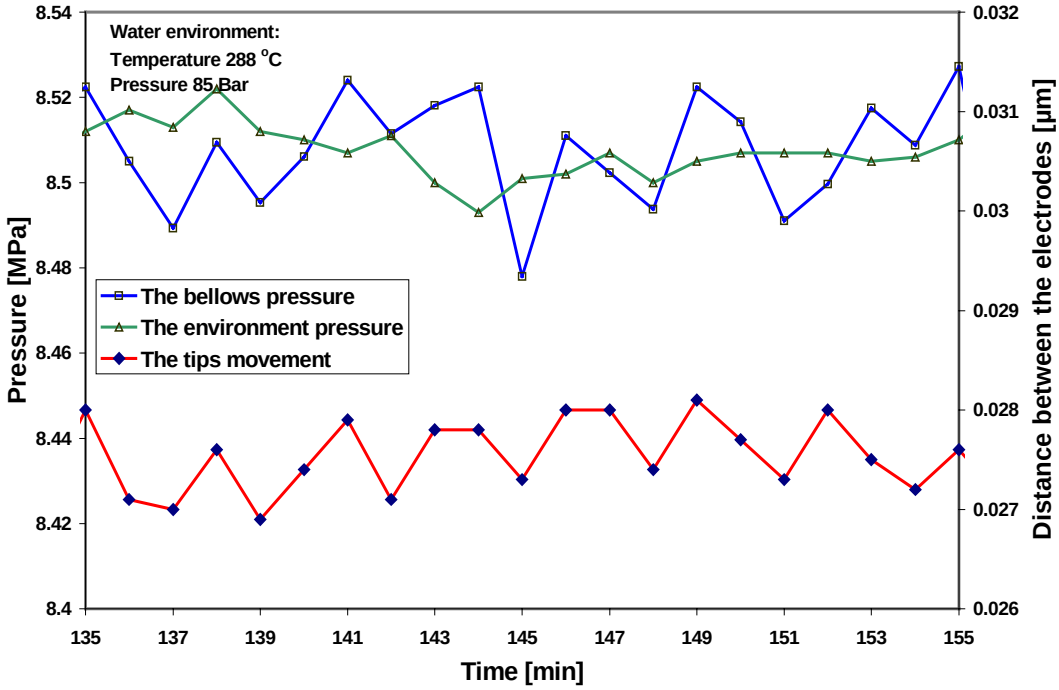

Figure 31. The distance between the electrodes, the bellows pressure and the environment pressure in a test made in a BWR environment under displacement control [8].

When the system is operated under pressure feedback control, the pressure variation of the environment can change the distance between the electrodes. The real pressure fluctuations in a typical static autoclave used at VTT are fairly low. However, the accuracy of the used pressure sensors causes a noise of ± 0.03 MPa. Using β = 0.1 mm/MPa, this pressure noise corresponds to a change of ± 3 μm in the electrode position. Due to the pressure variations, further development of the design was needed to be able to run experiments under pressure feedback control.

5.3.2 The bellows-driven CDE arrangement using pressure feedback control with additional springs and new software

On the basis of the preliminary tests described above, new arrangements for the adjusting programs and CDE spring stiffness were needed. The target of the experiments discussed in this chapter was to investigate how the increased spring stiffness affects the accuracy to control the distance between the electrodes. At the same time, the used software was re-designed and tested for the digital servo controller and CDE arrangement. The main parts of the new test set-up are shown in Fig. 32.

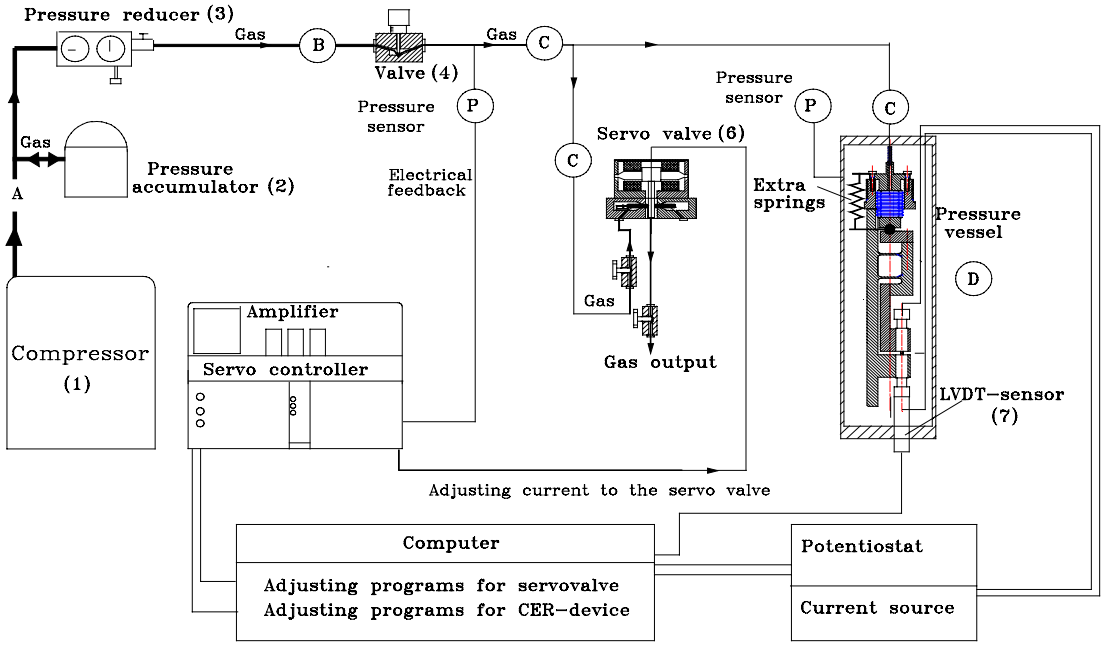

Figure 32. The test set-up for the pneumatic CDE arrangement working under pressure feedback control with additional springs and new software.

The new test set-up consists of controlling programs for the digital servo controller, potentiostat, current source and the data acquisition systems. To control the distance between the electrodes more accurately, additional springs were installed on both sides of the bellows in the CDE arrangement, Fig. 32. The calibration result using this CDE arrangement is shown in Fig. 33.

The stiffness of the new bellows arrangement was lower, and therefore

$$\beta = \frac{\Delta d}{\Delta p} = 0.0039 \ \frac{mm}{MPa} \qquad (2)$$

The distance between the electrodes can be changed from 0 to 0.034 mm (with a maximum of 8.6 MPa pressure difference between the environment and bellows pressures). As the environment pressure variation is typically ± 0.03 MPa, the distance between the electrodes varies roughly ± 0.12 μm due to external variations. This is quite acceptable for CDE measurements.

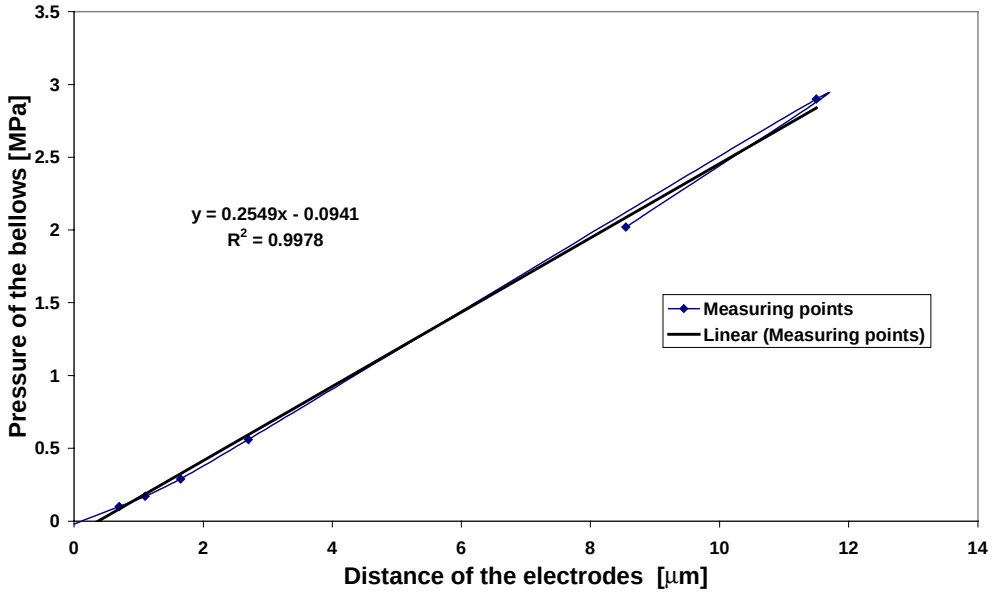

Figure 33. Distance between the electrodes in the CDE arrangement with the pneumatic bellows and additional springs attached at the sides of the bellows.

5.3.3 CER measurements with nickel electrodes in a gaseous environment at room temperature

The set-up presented in Fig. 32 was used to test the applicability of the system for CER measurements of nickel samples. In the beginning of the test, the electrodes with polished surfaces were pressed together resulting in a low resistance value (0.01Ω). After this, the bellows pressure was decreased until the electrode surfaces departed and the oxide film started to grow on the electrode surface. Then the bellows pressure was increased, the electrode surfaces were pressed together (with a nominal contact pressure of roughly 2 MPa), and a new contact resistance value was measured (roughly 1000 Ω). This measurement cycle was repeated to investigate how the contact resistance changes as a function of time. A typical measurement result is shown in Fig. 34.

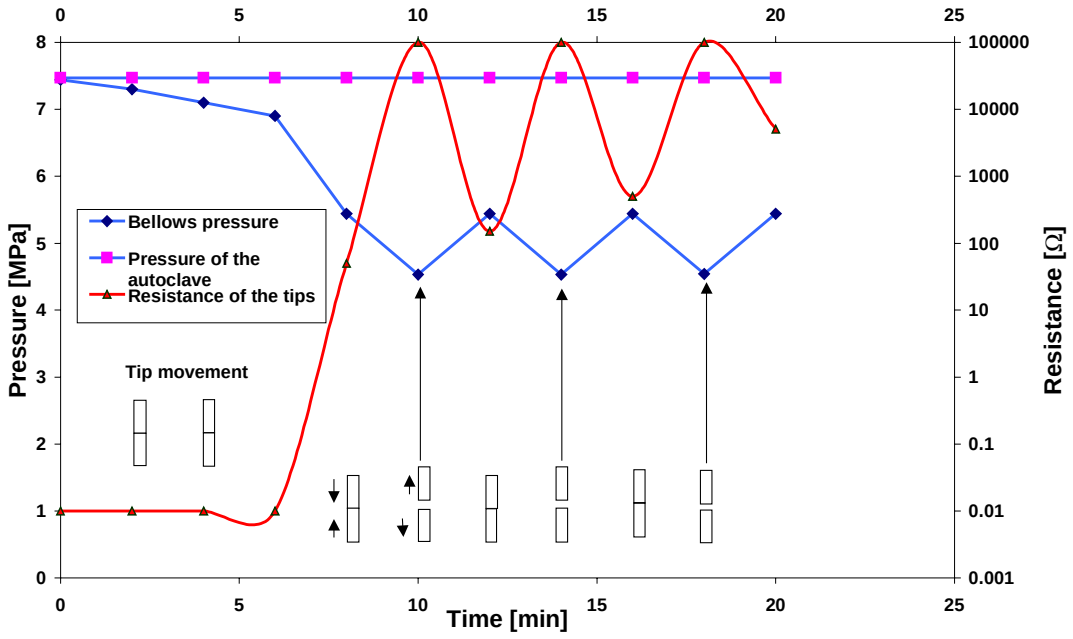

Figure 34. A scheme of the oxidation of pure nickel in a nitrogen/oxygen gas environment at room temperature.

Fig. 35 shows results from a CER measurement of nickel electrodes at room temperature in a nitrogen/oxygen gas environment, including the bellows pressure. In the beginning the bellows pressure was decreased slowly, resulting in a gradually smaller contact area of the polished electrode surfaces, and accordingly a slightly higher contact resistance. At about t = 2 min, the bellows pressure cycling was started so that at the higher pressure level (about 6.9 MPa) the electrode surfaces were in contact and thus not exposed to the gaseous environment. At the lower pressure level the electrode surfaces were exposed to the environment with oxygen in it, resulting in the oxidation of the surface layers (oxide growth) and a corresponding increase in the contact resistance. At the end of this test, the contact pressure was increased markedly, resulting in a significant decrease of the contact resistance. This may be due to the oxide film rupture or some other phenomenon.

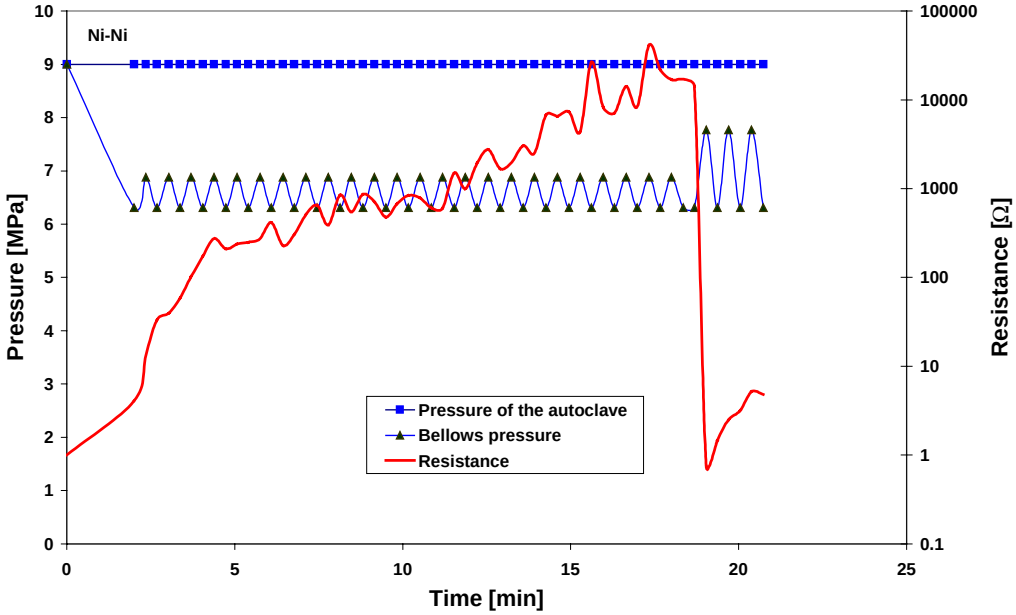

Figure 35. CER measurement of nickel electrodes at room temperature in a nitrogen/oxygen gas environment, showing also the bellows pressure.

An additional feature in the software developed is its auto-correction capability. In the test runs made in this study, the auto-correction function was found to work properly. During a long monitoring-type of measurement period the contact pressure may vary, due to changes in the temperature or pressure of the environment. Also the oxide film thickness may change during the test periods. Therefore, to be able to press the electrodes together using the same contact pressure throughout the test, the changes in oxide thickness need to be taken into account. At user selectable time intervals, the autocorrection function slowly changes the bellows pressure to the point where the first contact of the two electrodes is observed on the basis of the measured contact voltage value. In this way the contact pressure used in the measurement can be kept constant even during a long test run.

5.4 Summary and conclusions

The main conclusions concerning the optimisation of the bellows driven CDE arrangement reported in this work can be summarised as follows:

- The bellows-driven CDE arrangement developed can provide the required electrode distance control accuracy (± 0.2 μm) in a static autoclave where there is no pressure variation of the environment.
- The software developed for the bellows-driven CDE arrangement is at a stage enabling performance of the CER, CEI and TLEC measurements.

References

1. Saario, T., Laitinen, T. and Piippo, J. Contact Electric resistance (CER) technique for *in situ* characterisation of surface films. Materials Science Forum 193 (1998), pp. 289–292.

2. Bojinov, M., Laitinen, T., Mäkelä, K., Saario, T. and Sirkiä, P. Characterisation of material behaviour in high temperature water by electrochemical techniques. Enlarged Halden Programme Group Meeting, 15.–20. March 1998, Lillehammer, Norway.

3. Bojinov, M., Laitinen, T., Mäkelä, K., Saario, T. and Sirkiä, P. A combination of AC impedance and DC resistance techniques to study corrosion in high temperature aqueous environments. Proceedings of the 4th International Symposium on Electrochemical Impedance Spectroscopy, 2.–7.8.1998, Rio de Janeiro - Brazil, pp. 393–395.

4. Bojinov, M., Laitinen, T., Mäkelä, K., Saario, T., and Sirkiä, P. A novel technique for electrochemical measurements in low conductivity environments. EUROCORR'98, 28.9.–1.10.1998, Utrecht, The Netherlands.

5. Bojinov, M., Hinttala, J., Laitinen, T., Muttilainen, E., Mäkelä, K., Reinvall, A., Saario, T. and Suksi, S. Development of electrochemical techniques to study oxide films on construction materials in high temperature water. 1998 JAIF International Conference on Water Chemistry in Nuclear Power Plants, 13.–16.10.1998, Kashiwazaki, Japan.

6. Bojinov, M., Laitinen, T., Mäkelä, K., Mäkelä, M., Saario, T. and Sirkiä, P. Advanced electrochemical techniques for power plant use. EUROCORR '99, The European Corrosion Congress, 30.8.–2.9.1999, Aachen, Germany.

7. Bojinov, M., Laitinen, T., Mäkelä, K., Mäkelä, M., Saario, T. and Sirkiä, P. Optimisation and application of electrochemical techniques for high temperature aqueous environments. Enlarged Halden Programme Group Meeting, 24.–29. May 1999, Loen, Norway.

8. Moilanen, P., Arilahti, E., Bojinov. M., Laitinen, T., Mäkelä, K., Mäkelä, M., Mäkinen, R., Saario, T., Sirkiä, P. and Toivonen, A. Pneumatic servo-controlled fracture resistance measuring device (PSFM-device) and contact electric resistance measuring device (CER device). Enlarged Halden Programme Group Meeting, 24.–29. May 1999, Loen, Norway.

9. Bojinov, M., Laitinen, T., Mäkelä, K. and Saario, T. A study of the conduction mechanism in the passive film on iron using contact electric impedance and resistance measurements. Submitted to J. Electrochem. Soc.

10. Chechirlian S., Eichner, S., Keddam, M. Takenouti, H. and Mazille, H. Specific aspects of impedance measurements in low conductivity media - artifacts and their interpretations. Electrochim. Acta 35 (1990), p. 1553.

11. Beverskog, B. and Puigdomenech, I. Revised Pourbaix diagrams for chromium at 25–300 ^{o}C. Corrosion Science, 39 (1997), p. 43.

Published by

Vuorimiehentie 5, P.O.Box 2000, FIN-02044 VTT, Finland
Phone internat. +358 9 4561
Fax +358 9 456 4374

Series title, number and report code of publication

VTT Research Notes 2039
VTT–TIED–2039

Author(s)

Bojinov, Martin, Laitinen, Timo, Moilanen, Pekka, Mäkelä, Kari, Mäkelä, Matti, Saario, Timo & Sirkiä, Pekka

Title

Development of a controlled-distance electrochemistry arrangement to be used in power plant environments

Abstract

This publication presents the state-of-the-art of the controlled-distance electrochemistry (CDE) arrangement developed at VTT. Due to the possibility to control accurately the distance between two electrodes, the CDE arrangement makes possible electrochemical measurements in poorly-conductive media such as simulated coolants of light water reactor systems. This experimental arrangement has now been developed into a versatile electrochemical tool, which can be used for thin-layer electrochemistry (TLEC), wall-jet ring-disc and contact electric impedance (CEI) as well as contact electric resistance (CER) measurements. This report comprises results from the years 1997–1999 and summarises the different possible TLEC configurations and electrode locations as well as the development of a bellows-driven CDE system.

Keywords

controlled-distance electrochemistry (CDE), nuclear power plants, high temperatures, corrosion, measurement, fuel cladding, oxide films, water, experimentation, thin-layer electrochemistry (TLEC)

Activity unit

VTT Manufacturing Technology, Materials and Structural Integrity,
Kemistintie 3, P.O.Box 1704, FIN–02044 VTT, Finland

ISBN			Project number
951–38–5681–X (soft back ed.) 941–38–5682–8 (URL: http://www.inf.vtt.fi/pdf/)			
Date	Language	Pages	Price
July 2000	English	47 p.	A
Name of project		Commissioned by	
OXITECH		Finnish Ministry of Trade and Industry (KTM), Radiation and Nuclear Safety Authority, Finland, (STUK), OECD Halden Reactor Project, Norway	
Series title and ISSN		Sold by	
VTT Tiedotteita – Meddelanden – Research Notes 1235–0605 (soft back ed.) 1455–0865 (URL: http://www.inf.vtt.fi/pdf/)		VTT Information Service P.O.Box 2000, FIN-02044 VTT, Finland Phone internat. +358 9 456 4404 Fax +358 9 456 4374	